ระบบรอยแตกของเสาหินบะซอลต์บริเวณอำเภอวิเชียรบุรี จังหวัดเพชรบูรณ์

นางสาวจุฑามาศ เจริญสุข

โครงงานนี้เป็นส่วนหนึ่งของการศึกษาตามหลักสูตรวิทยาศาสตรบัณฑิต

ภาควิชาธรณีวิทยา คณะวิทยาศาสตร์ จุฬาลงกรณ์มหาวิทยาลัย

ปีการศึกษา 2559

FRACTURE SYSTEM OF COLUMNAR BASALT IN AMPHOE WICHIAN BURI, CHANGWAT PHETCHABUN

Miss Jutamas Charoensuk

A Project Submitted in Partial Fulfillment of the Requirements

for the Degree of Bachelor of Science Program in Geology

Department of Geology, Faculty of Science,

Chulalongkorn University

Academic Year 2016

Project Title	FRACTURE SYSTEM OF COLUMNAR BASALT IN AMPHOE WICHIAN BURI, CHANGWAT PHETCHABUN
By	Miss Jutamas Charoensuk
Field of Study	Geology
Project Advisor	Associate Professor Pitsanupong Kanjanapayont, Ph.D.

Submitted date.....

Approval date.....

.....

Project Advisor

(Associate Professor Pitsanupong Kanjanapayont, Ph.D.)

จุฑามาศ เจริญสุข:

ระบบรอยแตกของเสาหินบะซอลต์บริเวณอำเภอวิเชียรบุรี จังหวัดเพชรบูรณ์. (FRACTURE SYSTEM OF COLUMNAR BASALT IN AMPHOE WICHIAN BURI, CHANGWAT PHETCHABUN) อ. ที่ปรึกษาโครงงานหลัก รศ.ดร.พิษณุพงศ์ กาญจนพยนต์, 61 หน้า.

ระบบรอยแตกของเสาหินบะซอลต์ บริเวณอำเภอวิเชียรบุรี เป็นผลต่อเนื่องมาจากการ การชนกันของแผ่นพม่าตะวันตกกับแผ่นฉานไทยในสมัยอีโอซีนกระตุ้นให้เกิดการบางลงของเปลือกโลกและเกิดการแทรกดันตัวของมวลหินหลอมเหลวที่มีอุณหภูมิสูงขึ้นมาตามแนวรอยแตก ระบบรอยแตกรูปเสาหินเกิดจากการเย็นตัวของมวลหินหลอมเหลว

ลักษณะการตัดกันของรอยแตก และจำนวนด้านของเสาหินรูปเหลี่ยมสามารถบ่งบอกระดับความสมบูรณ์ของระบบรอยแตกได้โดยการคำนวณค่าตัวแปร ดัชนีหกเหลี่ยม, ค่าเฉลี่ยจำนวนด้านของเสาหิน และ ค่าอัตราส่วนแกนหลักต่อแกนย่อย จากการศึกษาลักษณะรอยแตกเสาหินบริเวณเสาหินดอนสวรรค์ ปรากฏว่ารอยแตกมีการพัฒนาดี มีค่าดัชนีหกเหลี่ยมเท่ากับ1.06 ค่าเฉลี่ยจำนวนด้านของเสาหินเท่ากับ 5.18 ค่าอัตราส่วนแกนหลักต่อแกนย่อยเท่ากับ 1.45 และค่าเฉลี่ยเส้นผ่านศูนย์กลาง เท่ากับ 40.59 เซนติเมตร ในขณะที่การศึกษาระบบรอยแตก บริเวณน้ำตกซับพลูพบว่าการพัฒนารอยแตกดีน้อยกว่าบริเวณเสาหินดอนสวรรค์ โดยค่าดัชนีหกเหลี่ยม เท่ากับ 1.33 ค่าเฉลี่ยจำนวนด้านเท่ากับ 4.93 ค่าอัตราส่วนแกนหลักต่อแกนย่อย เท่ากับ1.42 และค่าเฉลี่ยเส้นผ่านศูนย์กลางเท่ากับ31.30 เซนติเมตร การศึกษาลักษณะเนื้อหินภายใต้กล้องจุลทรรศน์แบบใช้แสง และการวิเคราะห์เคมีโดยวิธีเอกซ์เรย์ฟลูออเรสเซนซ์ พบว่าหินในพื้นที่ศึกษาทั้งสองพื้นที่สามารถจัดจำแนกให้เป็นหินแอปซาไรไคต์ ซึ่งเป็นหินชนิดอัลคาไลน์และยังสามารถจัดจำแนกให้หินที่เสาหินดอนสวรรค์เป็นหินชนิดแทรฟไฟต์และหินที่น้ำตกซับพลูเป็นหินชนิด แทรฟไฟต์ถึงทราไคต์บะซอลต์จากการพล๊อตกราฟแอลคาไลน์กับซิลิกา

ลักษณะของระบบรอยแตกเสาหินเหล่านี้สามารถใช้เชื่อมโยงกับลักษณะของหินอัคนีที่เป็นชั้นกักเก็บปิโตรเลียมในแหล่งวิเชียรบุรี และสามารถประยุกต์ใช้ในการสำรวจปิโตรเลียมต่อไป

ภาควิชา ธรณีวิทยา ลายมือชื่อนิสิต_____

สาขาวิชา ธรณีวิทยา ลายมือชื่อ อ.ที่ปรึกษาหลัก_____

ปีการศึกษา 2559

5632704423 : MAJOR GEOLOGY
KEYWORDS: COLUMNAR JOINT, WICHIAN BURI BASALT, COLUMNAR BASALT

FRACTURE SYSTEM OF COLUMNAR BASALT IN AMPHOE WICHIAN BURI, CHANGWAT PHETCHABUN. ADVISOR: ASSOC. PROF. PITSANUPONG KANJANAPAYONT, Ph.D., 61 pp.

Columnar joint in Aumphur Wichian Buri is Cenozoic basalt formed as a consequence of continental collision between Western Burma and Shan-Thai. This collision in Eocene have triggered the thinning of the crust and the intrusion of high-temperature basaltic magma along the weakness zones. Columnar joint is formed when hot lava masses cooling.

The intersection type and the polygon-side number can be indicated the maturity of joint by calculating some parameters including hexagonality index, average number of side, and axial ratio. By calculating these parameter, columnar joints at Sao-Hin Donsawan are well developing which yield hexagonality index 1.06, average number of side is 5.18, the axial ratio is 1.45, and the average diameter size is 40.59 cm; whereas, columnar joints at Sub-Phlu waterfall are not very well developing and yield hexagonality index 1.33, average number of side 4.93, the axial ratio1.42, and the average diameter size is 31.30 cm. Furthermore, the rock in both study areas can be classified into absarokite, alkaline series based on texture observation under microscope, XRF data, and CIPW Norm calculation. By using the total alkali versus silica (TAS) diagram, the rock can be classified into Tephrite at Sao-Hin Donsawan and Tephrite to Trachy-basalt at Sub-Phlu waterfall.

These characteristics of columnar joint and rock type may relate to the fracture system in the igneous reservoir rock in Wichian Buri petroleum field which lead to the supplement data in petroleum exploration.

Department : Geology Student's Signature_____

Field of Study : Geology Advisor's Signature_____

Academic Year : 2016

Acknowledgment

I would like to thank my senior project advisor Associate Professor Pitsanupong Kanjanapayont of the department of geology at Chulalongkorn University. He allowed this paper to be my own work, and lead me in the right the direction to fulfill my project report.

I would also like to specially thank the Dr. Abhisit Salam and Dr.Piyapong Chenrai of the department of geology at Chulalongkorn University who were involved in this research project to guide me and give me suggestion for the report writing.

I would to thank Mr. Suwat Makjareun who was involved in the survey for this senior project. Without their passionate participation and input, the validation survey could not have been successfully conducted.

Content

List of Tables

List of Figures

Unit 1

Introduction

1.1 Background

1.1.1 Columnar joint

Columnar joints, polygonal pattern of cracks, show the long-slender columns in bodies with vary side and shape. These joints typically form in basalt. Natural polygonal fracture system in basalt, also known as columnar basalt, is a charismatic characteristic in basalt flow which occurs by contraction during cooling and develops pattern of fracture in the igneous bodies.

Glossary of geologic term descripted the term of columnar jointing in 2016, “Columnar jointing is the type of jointing that breaks rock, typically basalt, into columnar prisms (Glossary of geology, 2016). Usually the joints form a more or less distinct hexagonal pattern.”

1.1.2 Columnar basalt in Thailand

There are 4 sites of columnar basalt in Thailand.

1) Amphoe Wichian Buri, Changwat Phetchabun

Wichian Buri basalt is fine-grained porphyritic rock. Some areas developed columnar structure, and some columns are inclined with different angle. The age of the rock is about 11million years ago. (Sutthrat et. al., 1994)

2) Ban Na Phun Pattana, Amphoe Wang Chin, Changwat Phare

This columnar basalt formed in 5-6 million years ago (Wattanakul, 2006).There are 7-8 piles of columnar basalt which mostly composes of pentagonal and hexagonal column. The diameter of columnar basalt is about 35 cm, and the column height is between 5-10 m over the ground surface. By geophysical survey, the igneous columnar body thickness is between 10-30 meters deep in the ground. Some of columns are inclined and some are perpendicular to the earth surface. (Wattanakul et al., 2006)

3) Wat Sand Tum, Amphoe Khoa Saming, Changwat Trat

More than hundred columns neatly arranged perpendicular to the earth surface. The average diameter is about 30 cm. The side of the column is varies from 3 to 12 sides. These columns are basalts which compose of

black aphanetic texture with black spinel phenocryst. The age of this rock is about 1milloin year ago. (Department of mineral resource, 2013)

4) Phu Eung Kan, Tambon Nang Rong, Changwat Burirum

Phu Eung Kan basalt came from the lava intruded in the fissure around the volcano. These lava temperature ranges from 700 to 1200 degree celsius. The lava has low silica content and low viscosity, thus the lava flows over broad area. The age of volcano explosion is about 700,000 years ago (Department of mineral resource, 2011).

All of these columnar basalts formed in Late Cenozoeic. These basalts have different character. Due to very few studies of columnar structure in Thailand, geological data and development of these columnar basalts are poorly understood. The understanding of columnar structure yields a lot of application in other countries. For example, the use as a nuclear disposal waste in Columbia River site basalt in USA and Parana Basin basalt in S.E. Brazil (Olalla et al., 2010) and use for high-arch dam foundation (Wei et al, 2011).

Wichian Buri rock unit has a significant benefit to put an attention on. It is important to petroleum industry, since there are igneous reservoirs of waxy oil in Wichian Buri petroleum field (Dejtrakulwong, 2014). This is an excellent example for igneous reservoir in Thailand. The study of this rock in the study area must improve the understanding of geological data and may be applied on exploration of petroleum field. Therefore, Wichian Buri columnar basalt has distinct benefit in petroleum field and is the most interesting columnar basalt.

1.1.3 The Late Cenozoic Basalts in Thailand

The Late Cenozoic basalt in Thailand occurs as small vents and distributed over the Northern and Upper Western highlands, Khorat Plateau, the Eastern Region, and Loei- Phetchabun Ranges. The distribution is controlled by topographic and structural geology of the areas as shown in figure 1

The Late Cenozoic Basalts in Thailand were dated by several research ranged from 24 Ma to less than 0.5 Ma (Sutthirat et al., 1994; Sutthirat et al., 1995; Boonsoong, 1997; Chualaowanich et al., 2008). These basalts might be erupted in continental rift which were the results of fracture opening during collision of Indian and Eurasian plates (Jungyasuk and Kositanont, 199s; Smith, 1996).

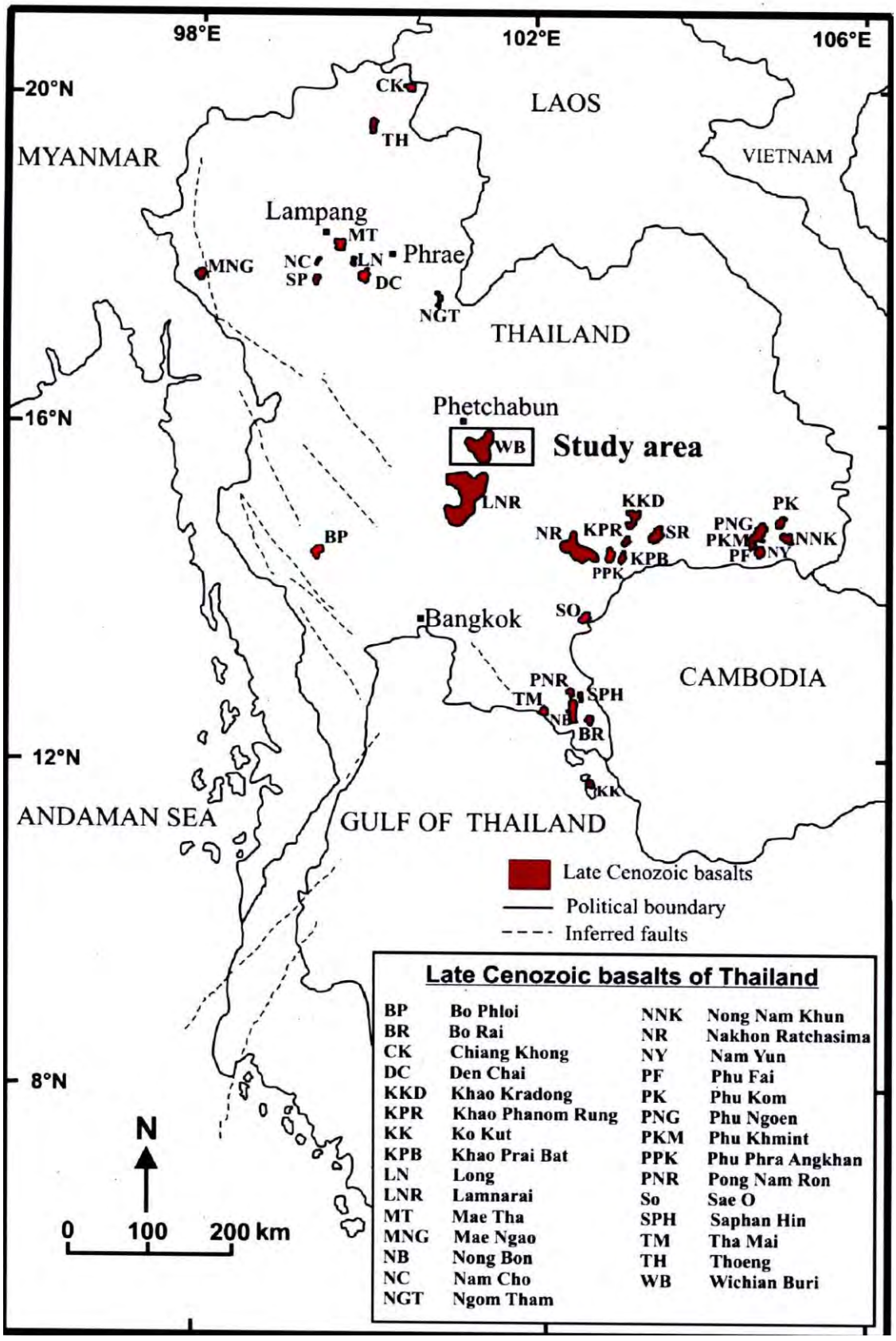

Figure.1 Map shows the location of late Cenozoic basalt in Thailand (Limtrakul et al., 2005)

1) Wichian Buri Basin

Wichian Buri basin is one of Phetchabun sub-basins formed through transtensional dextral shear along Mae Ping fault zone in Late Oligocene. Its structures is half-graben structure mainly N-S trend with secondary NE-SW trend east bound half-graben in south and changes to west bound half-graben in the North. Maximum depth is 2500 meter. Alluvial sediment and fine grain volcanic sequence overlade Permo-Triassic metasediment in Late Oligocene. During Late Oligocene to Middle Miocene, organic-rich lacustrine shale which is the source of hydrocarbons deposited interfingering with thin bedded deltaic sands, called Wichian Buri Group. Igneous bodies were widespread with in Wichain Buri sub-basin including fine-grained syn-rift volcanics, Lower and Middle Miocene diorite and diabase intrusive bodies, Lower Miocene basaltic tufts, and Pleistocene basalts which formed in the northeast of the Wichian Buri sub-basin and extended surficial sheets to the south of the basin. After the Mid-Miocene tectonic episode, lacustrine conditions were widespread over the basin and resulted in fine-grained sediments deposit, called Chaliang Lab Formation. Relative subsidence in Pliocene established fluvial environment to Pleistocene which yielded lithic sands and shale deposition in an oxidizing alluvial environment (Remus et al., 1993). Oil field at Wichain Buri basin is an example of hydrocarbon reservoir associated with igneous intrusion.

Based on lithostratigraphic and biostratigraphic data, igneous rocks in Wichian Buri basin can be divided into two groups. The first group emitted lower gamma radiation and another group emitted higher radiation. Mafic intrusive and tuff, mainly composed of plagioclase, pyroxene, and hornblende are the first group which emit lower gamma radiation. Another group emitted higher radiation is intrusive rocks composed of K-feldspar and biotite (Webster et al., 1990). The mafic volcanic rock in Wichian Buri basin is underlain by Permian and Tertiary strata (Jungyusuk and Sinsakul, 1989).

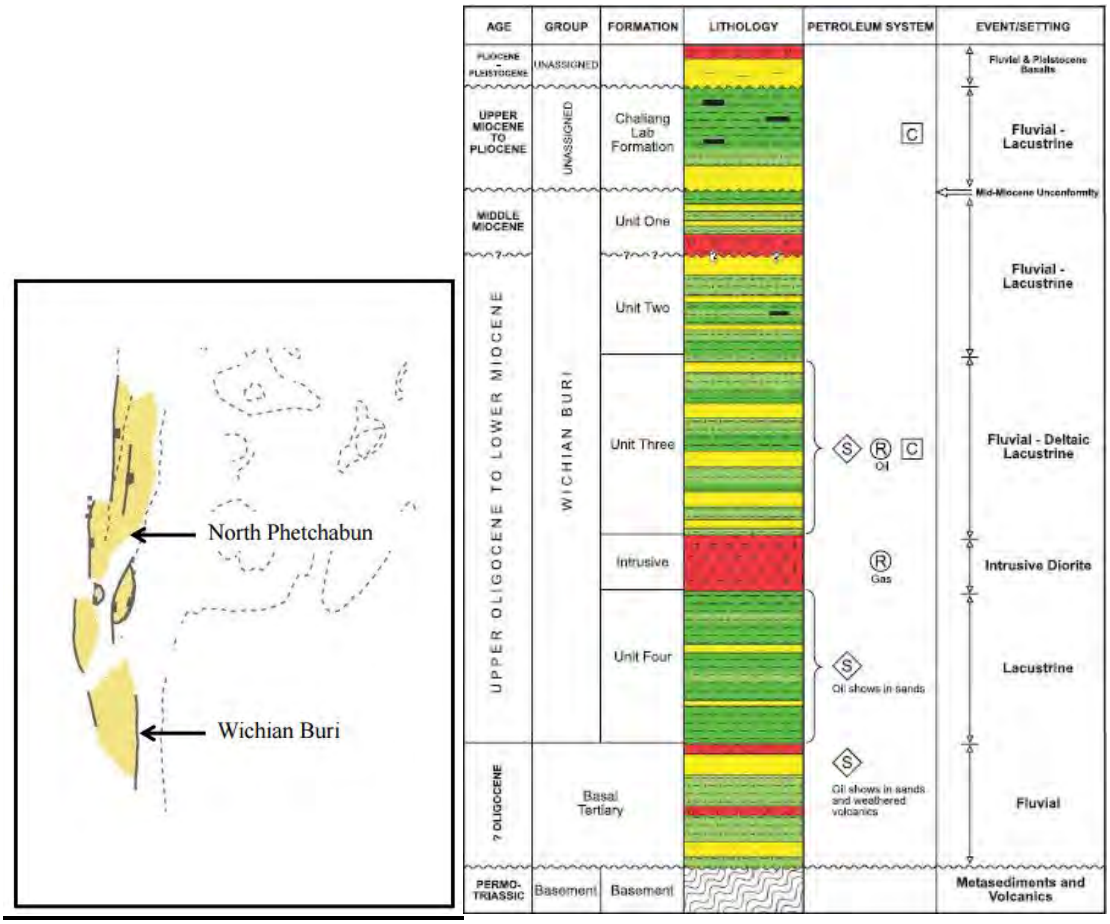

(a) (b)

Figure. 2 (a) Map of Wichian Buri basin. (b) Stratigraphy in Wichian Buri basin (Dejtrakulwong, 2014 and Williams et al., 1995)

2) Wichian Buri basalt

Wichian Buri basalt is Late Cenozoic basalt which flowed in Amphoe Wichain Buri Changwat Petchabun, Thailand. This basalt covers approximately 200 km^2. Wichian Buri basalt was ranged in 8.73-11.6 Ma by radiometric dating, Ar-Ar method, showing in table 1(Charusiri, 1989; Intasopa, 1993; Sutthirat et al., 1994; Sutthirat et al., 1995a; Chualaowanich et al., 2008).

Table 1. Age of Wichian Buri basalt from many research, dating by radiometric dating, Ar-Ar method

Name(year)	Age (million year)
Charusiri (1989)	9.7-11.6
Intasopa (1993)	9.08+/- 0.29
Sutthirat et al. (1994)	8.82+/- 0.09
Sutthirat et al. (1995a)	11.03+/- 0.03
Chualaowanich et al. (2008)	9.84+/- 0.06

Wichian Buri basalt is composed of two lava flows (Vichit et al., 1988). The first is coherent basalts flows which composed of fine-grain porphyritic rock and partially columnar joints; some are dark gray, grayish, and black color. The components of this type are vesicular with amygdale quartz, chalcedony, zeolites, and calcite. Some are intruded by mafic hypabyssal rock (Sutthirat et al., 1994). These basalts may have lherzolite and ultramafic nodules, spinel, xenolith, and corundum. Another type is incoherence facies composed of basalt breccia which is poorly sorted, angular to rounded mafic volcanic fragment, and fine-grained-glassy matrix. Wichian Buri basalt is geochemically classified as alkali basalt (Sutthirat et al.,1994).

1.2 Importance

There are many prominent columnar basalt sites in Amphoe Wichicn Buri, Changwat Phetchabun. These columnar basalts are still unclear because of few studies in the area. Few studies of Cenozoic basalt in Wichian Buri basin are about the age and the petrography of basalt, not directly mention to the columnar basalt. To understanding the origin of columnar basalt and the characteristic of columnar joint may yield importance geological data.

Petroleum exploration and production companies are also interested in this region because of the occurrence of oil. Wichian Buri basin is an important Petroleum field in Thailand and the production rate in the field, L16/57A and L16/57B, is 4,336 pbd and is estimated to contain 30 MMbbl of waxy oil (Dejtrakulwong, 2014). Hydrocarbon reservoirs in this area associated with igneous intrusions which relate to late Cenozoic basalt, Wichian Buri group. The petroleum system in this area may be somehow correlate to the fracture system in columnar basalt on the surface.

1.3 Purpose of study

1.3.1 To study characteristics of columnar basalt in study area.
1.3.2 To understand how columnar basalt form in the area.

1.4 Study Area

There are two study areas in Amphoe Wichain Buri, Changwat Phetchabun. Study area 1 is located in Tambon Khok Prong Amphoe Wichian Buri Changwat Phetchabun, Thailand. Study area 2 is located in Tambon Yang Sao Amphoe Wichian Buri Changwat Phetchabun, Thailand. The distance between these two

areas is around 5 kilometers. The study area 2 is located to the North of study area 1, as shown in figure3.

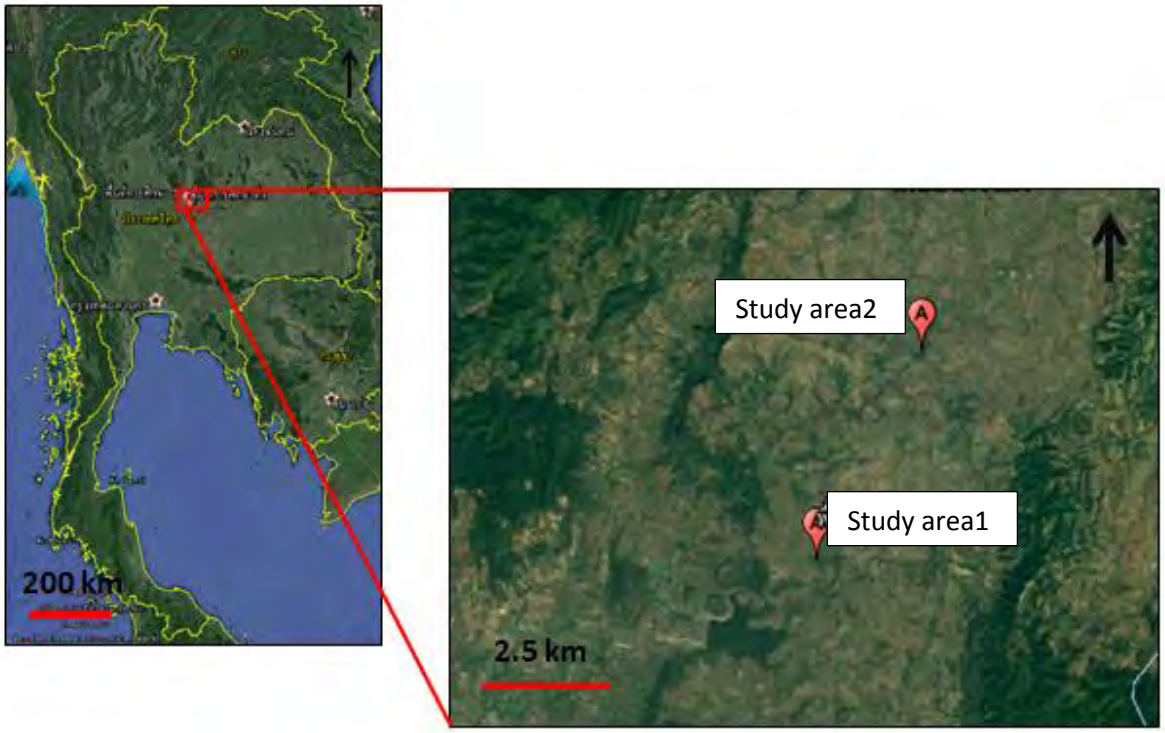

Figure.3 Location study area 1 and study area 2

1.4.1 Study Area 1

Grid UTM WGS84 Zone47P Easting741643 Northing1748175

Sao-Hin Donsawan House of priest, Tumbon Khok Prong Amphoe Wichian Buri, Changwat Phetchabun. This area is channel, natural outcrop, 20 meters long and 4 meter high. This area is shown in figure 4.

Figure.4 Columnar basalt outcrop of study area1

1.4.2 Study Area 2

Grid UTM WGS84 Zone47P Easting746283 Northing1756206

Sub-Phlu waterfall Tumbon Yang Sao, Amphoe Wichian Buri, Changwat Phetchabun. This area is waterfall, natural outcrop, 10 meters long and 3 meter high. This area is shown in figure 5.

Figure.5 Outcrop of columnar basalt of study area2

1.4.3 Accessibility of Study Area

From Chulalongkorn University, go to the north along PayaThai road, then drive along the Paholyothin road about 120 km. When arrive at Pukae, Amphoe Chaloem Phra Kiat, Changwat Saraburi, at intersection, turn to the road no. 21, drive about 150 kilometers. At the Rahun junction (Phetchabun), go to the East to the road no. 225, drive about 25 km. Then turn to the north along the rural road about 3.5 kilometers, you find the Haui-Leng reservoir, drive along the reservoir to the northeast about 3 kilometers you will see a small road to the Sao-Hin Donsawan House of priest, go through the small road about 500 meter to Sao-Hin Donsawan House of priest. This is study area 1.

From the study area 1, drive back the same way to the road no.225. Then go to the East along the road no.225 around 12 kilometers. Follow the sign to the Sub Phlu waterfall. Turn to the north along the rural road about 8 kilometers. You will reach Sub Phlu waterfall. This is study area 2.

1.5 Expected results

1) Understanding of fracture system and characteristics which may lead to understanding of relationship of petroleum system in study area.

2) Knowing the origin of columnar basalt and fracture system in Amphoe Wichian Buri.

1.6 Process planing

Table 2. Process planning schedule

	Aug	Sep	Oct	Nov	Dec	Jan	Feb	Mar	Apr	May
Literature Review										
Collecting Field Data										
Compute &Analysis										
Interpret data										
Writing Report										
Presentation										

Unit 2

Literature Review

2.1 Columnar basalt

Columnar basalt is one of the most prominent characteristics of basalt flow. At the surface of basalt flow, there may be some textures which indicated that the lava flow get in touch with atmosphere such as the Pahoehoe or ropy lava strucute, vesicular texture, and Aa or blocky lava. The columnar jointing migh be overlaid by these characters on the top of upper column. As the lava masses continue cooling, the contraction on the surface of basalt increase and develop the joints when the contraction stress is more that the cohesive force of the rock. The structure of the columnar flow on the ground surface is shown in figure 6.

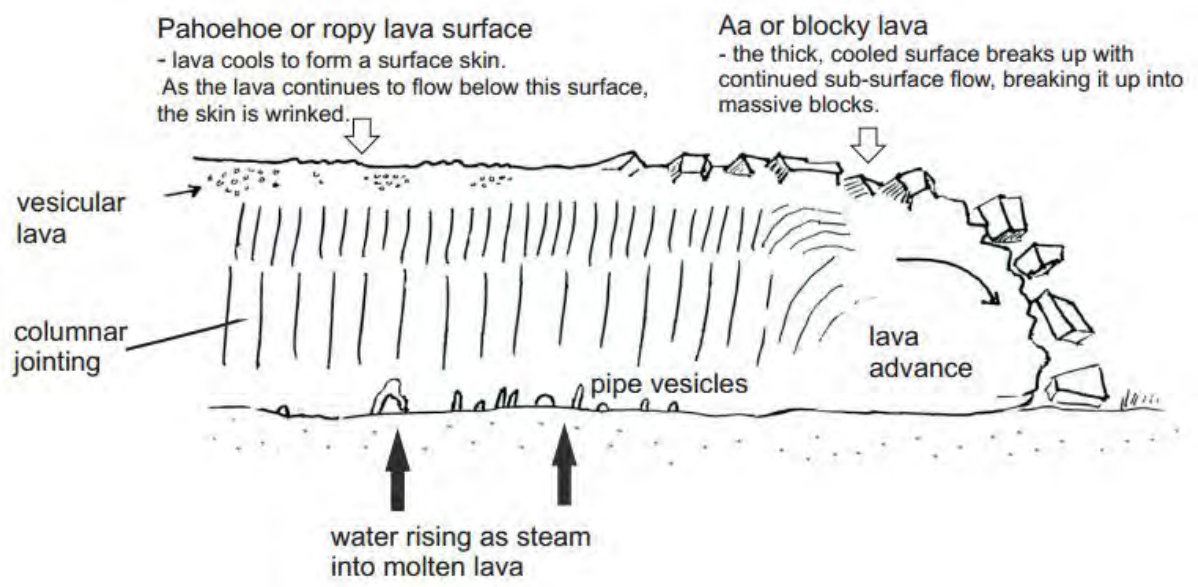

Figure 6. The structures of basalt flow on the ground surface
(from: www. esta-uk.net/index_htm_files/Basalt_Lava_Flows.pdf)

As the cooling progress, the cooling causes contraction and develops joints. In cooling process, there are many cooling centers which are the highest- temerature points compare to the other points around them. The cooling prograde directly toward the centers and that made the cooling centers in the middle of the columns when the lava cool down. Because, the contraction tends to prograde directly toward each center on the surface, the cracks develop in between each pair of the cooling centers as shown in figure7. The cracks distribute over the surface and growth down to the area under the surface. Normally the column are perpendicular

to the cooling surface. However, if there are any pressures or lava movements, the columns may bent over.

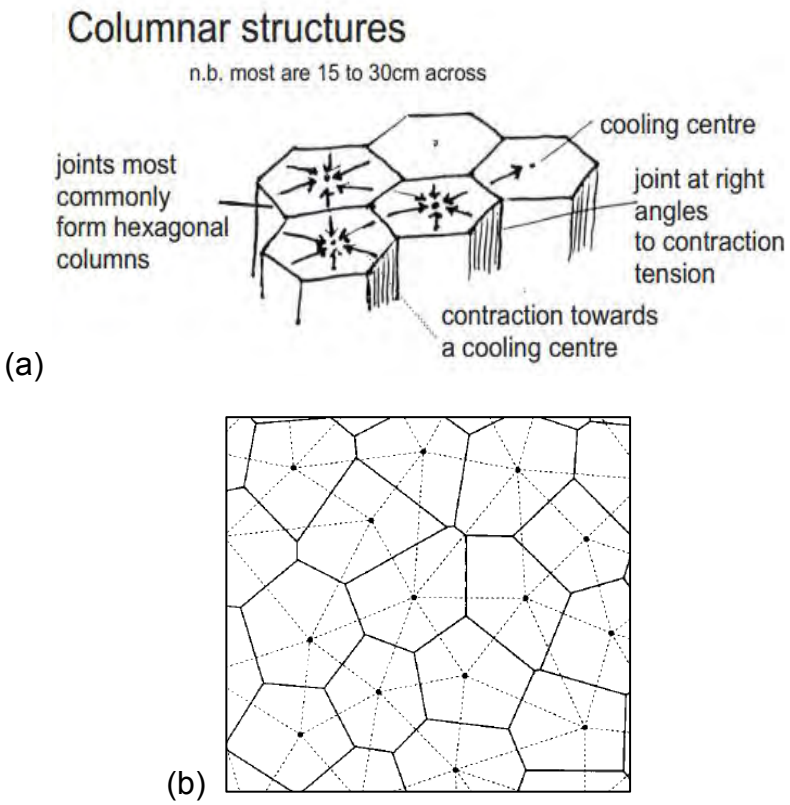

Figure 7. (a) Cooling center in columnar basalt
(from: www.esta-uk.net/index_htm_files/Basalt_Lava_Flows.pdf)
(b) The cracks develops in the middle of two cooling centers (Budkewitsch and Robin,1994)

2.2 Structure of columnar basalt flow

Columnar basalt flows are composed of two or more layers. Each layer is called tier and can be categorize into two characters, colonnade and entablature.

Colonnade is a tire of columnar joint which is perpendicular to boundary. The columns arrange neatly and perfectly. This type of tier is tabular cooling geometry. The columns in the top flows propagate downward, whereas the columns in basal flow propagate upward.

Entablature is narrow, curved, and fanning columns. These columns do not arrange neatly. The columns are not parallel to one another. This tire is often found between upper colonnade and lower colonnade.

In thin basalt flows, there are usually two tires composed of upper colonnade and lower colonnade. These two colonnades meet at quasi-planar interface which are distinguished by the mismatch of upper colonnade and lower colonnade joint set

(Budkewitsch and Robin, 1993). The structure of columnar basalt flow is shown in figure 8.

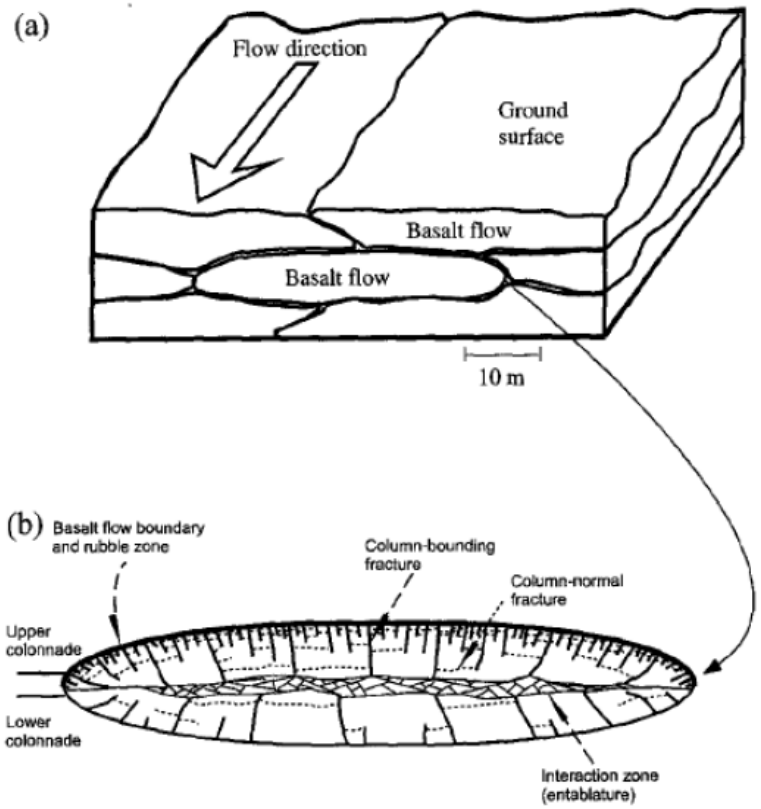

Figure 8. (a) Character of lava flow in the layer. (Lore et al., 2001)
(b) Structure of columnar basalt flow after cooling (Lore et al., 2001)

2.3 Cause of columnar structure by Albert V. G. James (1920)

Geometry of columnar basalt including size and shape depends on various factors. For example temperature of the lava, viscosity of the lava, the rate of cooling, the regularity of cooling, the homogeneous of the lava

The contraction due to cooling mainly controls formation of columnar joint. When the rock cools, it contracts and is subjected to tension. When the tension is greater than the power of extension, the cracks propagate. Considering the lava flows, it is cooling from surface, at the beginning. So that, the lava surface cools quickly from the convection current above the surface (in the air above surface). Then the solid forms at the surface of lava flows. The lava under the solid crust cools slowly because this solid crust is very poor heat conductor. The crack extends down to the lava until the power of tension equal to the power of extensions, only a short distant. In deeper lava, the rock is subjected to both vertical and horizontal tension. Vertical tension, from the solid crust on top, does not cause cracks but horizontal does. The temperature of cracking is between 315 degree Celsius to 500 degree Celsius and the temperature is lower when the rate of cooling is slow (Mallet, 1875).

The solidification and shrinkage of rock are caused by cooling and crystallization. The complete crystallization is developed in the slow cooling which yields great contraction. In fact, olivine crystals, gases, and other mineral are segregated during the cooling and these made lava masses heterogeneous. Perfectly homogeneous lava made the joint separate in equal area of columnar. The polygonal areas tend to be hexagon more than other shapes. The size of column depends mainly on temperature and rate of cooling. The more rapidly cooling rate produces the thinner column.

James (1920) believed that molten basalt cools slowly since it has low thermal conductivity. If columnar basalt is not developed well, basalt lava may either heterogeneity or rapid cooling of thin flows. The cracks in basalt start in hot solid rock when the contraction is larger than the expansion. The maximum rate of cooling is at the surface and the rate of cooling controls size of column. The upper most layers may not be column but fragment, ropy, or scoria. In this case, cooling is too rapid to form column. In some rock section, glass texture may be found. Moreover, column may be form from two cooling surface, the top surface and floor surface. The upper surface cools by air convection current and convection along the vertical joint, this section is rapidly cool. The lower section cools slowly because it only losses heat by convection at the bottom surface and the conductivity of the rock is very low.

Isothermal plane in upper layer are packed closer than lower layer. There are two set of column form, the upper column is thin, long, and irregular but the lower column is short, thick, and more perfect. The upper column is more heterogeneous because there are some movements, gases erupts, volcanic rains, and surface water.

Bent columns are formed when isotherms are not parallel to one another. The columns bend into the most rapid cooling. The change of direction dues to the presence of gas, water, etc. ; the irregularities in valley floor; the warping of the lava‟s upper surface; the scoriaceous or vesicular surface; convection current in lava; rain form volcano; chemical component in lava that effect the thermal conductivity.

2.4 Modelling the evolution of columnar joint by Paul B. and Pierre-Yves R. (1993)

Cooling cracks are developed from the cooling of lava flows, intrusive dikes, and sills. The cracks propagate inward the lava masses and develop to columnar structure on the surface. At first, initial crack pattern at the surface is not pseudo-hexagonal pattern but it evolve later. The columnar develop step by step, by repeating step wise crack, forming from centemeters to decimeters. This process

leaves the traverse band on the side of columnar structure. In well develop columnar, polygonal structure shifts sligthly from crack to one another.

Columnar joint is the thermal cracks which is perpedicular to the maximum tensile stress. The cracks propergate perpendicular to isothermal plane and propergate into the lava masses. The cooling begins from both surface of the lava masses , the upper surface and the bottom as shown in figure 9. The principal tensile stress is parallel to the isothermal suface and flow contact surface. The cracks is perpendicular to the flow contact because of tensile stress.

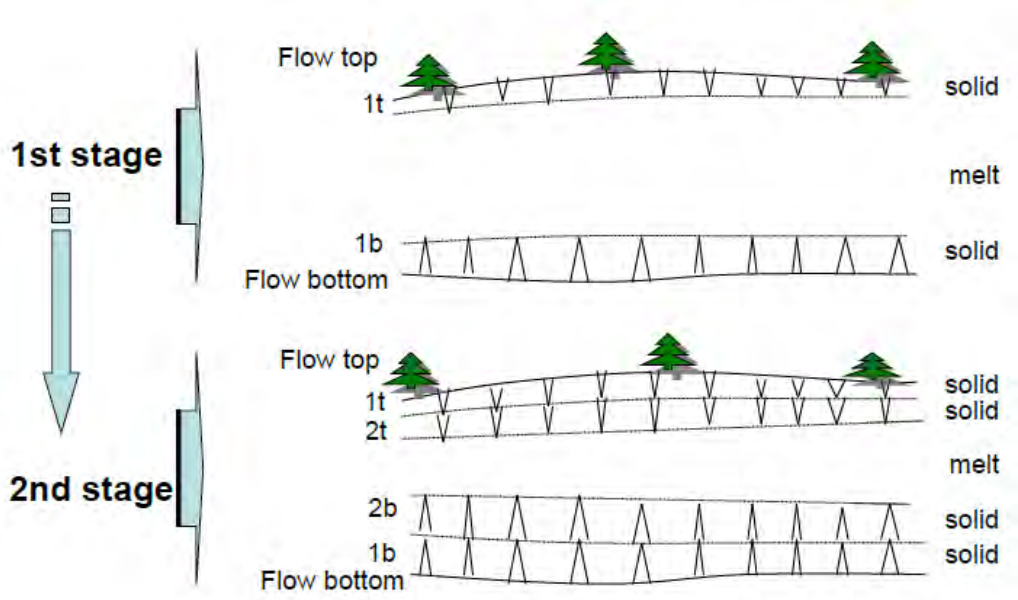

Figure. 9 Conceptual model of cooling, thermal stress generation, and fracturing. (DeGraff and Aydin, 1987)

It is believed that cracks are parallel to the highest thermal gradient. If there are some different size of columns, there are assymmetry isotherms at that area. The new cracks will propagate toward the biggest and hottest column.

The colums are convex and irregular polygon with various sizes, but pentagon and hexagon are predominant. Budkewitschand Robin (1993) studied model and algorithym of columnar basalt, believed that the evolution of columanar basalt initailly start as an immature crack pattern to the mature crack pattern, a pseudo-hexagonal which the average number of sides is about six as shown in figure 10.

In immature crack pattern, the X-type crack junction is predominant, whereas Y-type junction is found in mature crack pattern. Rapid evolution of crack in cooling lava yields equal size of column. The change of cooling and diverging of growth can be observed along the side of column. Band striaes or chisel marks on the side of column are the result of the increment of cracks which record tensile stress during the cooling. Plumose structure implies kinematic of crack nucleation and crack

propagation. Each column is a stack succession of short crack segment. Crack advance propagate when tensile strength at the tip of joint is greater than tensile strength of rock. The crack continues generating until the isotherm of rock equals to the glass transition temperature. The distances of each crack is lower following the function of thermal gradient. If the column diameter is smaller, the height of band on the side of column will be higher.

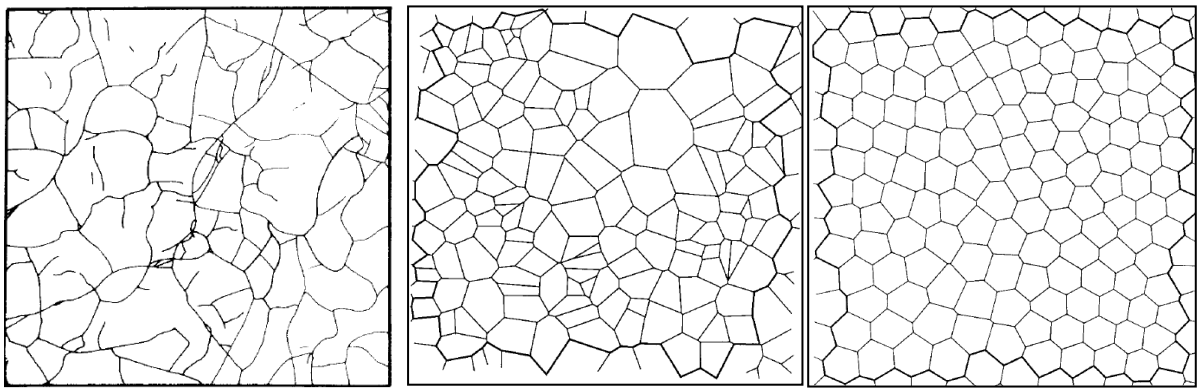

Figure. 10 Evolution of immature cracks to the mature cracks. (a) is immature cracks, (b) is the intermediate stage of cracks, (c) is mature cracks. (Budkewitsch and Robin, 1993)

2.5 Convection and conduction heat transfer in columnar basalts

Cooling front is deep in the surface lossed heat by two processes. The first process is heat conduction toward the cooling joints, and another process is convection out of flow through conduit (joint). Convection media normally invloves with water and vapor. Heat convection transports parallel to the colum axis (perpendicular to the contact of lava flow). However, the convection can be complex by the convection of water, dehydration of underling material, and other factors. The length and size of column subjects to the efficientcy of convection. These theory of convection and conduction have variety evidance including the direct field observation in Hawii lava lake(Hardee, 1980), data on glass transition (Sammis, 1981), and mathematical models (Hardee, 1980)

In column, the interior rock is hotter than the surfaces of joint which is shown in figure 11. According to the model, the cooling time of the lava flows is a linear fuction of the initial of the cooling at the surface of lava. The cooling rate is inversely to the fuction of column size. The heat lossed rate decreases when the column diameter increases. If the upper colonade is short and the diameter is large, the rate of cooling is slow, in dry condition. If the lower colonade is long and the diameter is small, the cooling rate is high, in dehydration of mudstone underling. The thick upper entablature, glass texture, and thin lower collonade imply theconvection of water associated to lava flows.

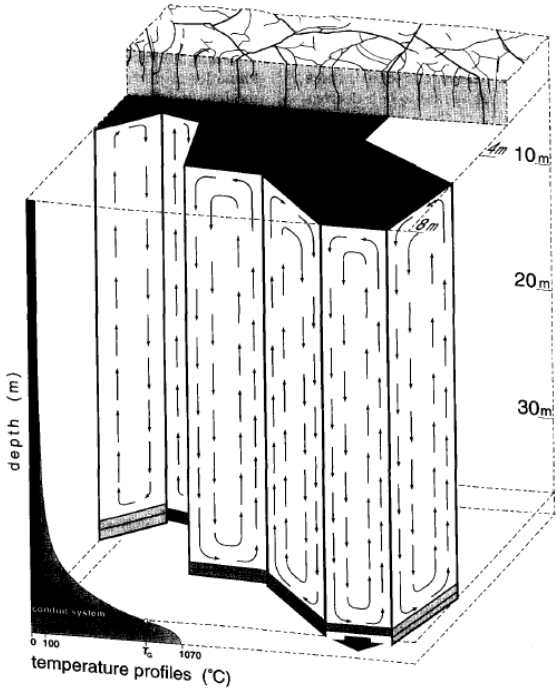

Figure. 11 Convection along the joint shows the cooling crack advance downward. (Budkewitsch and Robin, 1994)

2.6 Geometry of columnar joint

The joint set at the surface of cooling basalt lava is interlocking polygon and is similar to mosaic pattern as shown in figure12. Hexagonal is the best effective pattern to release tensile strength in cooling lava. Ideally, columnar basalts develop to hexagonal columns. However, three to eigth side polygonal columns can be found in the cooling lava. Pentagonal and hexagonal columns is the most number.

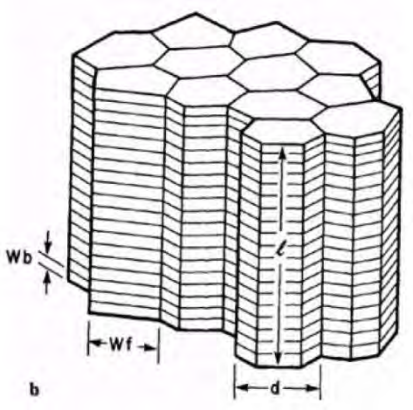

Figure. 12 Drawing of columnar basalt character. Symbols represent column length (l), column diameter (d), column-face width (Wf), band width (Wb). (DeGraff and Aydin, 1987)

2.6.1 Average number of sides

Average number of sides per polygon is defined by n:

$$n = 2(2J_T+3J_Y+4J_X)/(J_T+J_Y+2J_X)$$

where J_T is a fraction of number of T-type intersection to all type of intersection, J_Y is a number of Y-type intersection, and J_x is a number of X-type intersection.

It is believed that if T-type intersection is dominant, n-number is approximately 4. If the Y-type intersection is dominant, the n-number is nearly 6. This n-number indicates the crack pattern type.

2.6.2 Hexagonality Index

Hexagonallity index is definded by X_N;

$$X_N=((f_5+f_7)+4(f_4+f_8)+9(f_3+f_9)+16f_{10}+25f_{11})^{1/2}$$

Since the polygonal columns are 3-8 side polygon, the formular adjusts to

$$X_N=(f_5+f_7+4(f_4+f_8)+9f_3)^{1/2}$$

Where f_n is the function of n-side polygon. fn= n-side polygon divides by a sum of all polygon. As the columnar joint growth and mature, lower number-side polygons tend to be six sides and X_N tends to 0.

2.6.3 Axial ratio

Axial ratio is definded by the ratio of the largest axis divided by the shortest axis. This formular is made for any shape that has two or more axis. In mineralogy, axial ratios are the relatives lengths of crystal faces. Normally, the ratio of the length of each axis is divided by the length of b axis (a/b:b/b: c/b).

For measurment of maturation in columnar basalt, Paul B. and Pierre-Yves R. (1993) used Axial ratio to study the distribution of fractures that forming polygon. For each polygon must has a best-fit ellipse which has ratio of interior tenser equal to the polygon. axial ratio is defined by r;

$$r=a/b$$

where a is major diameter of the best-fit ellipse and b is minor diameter of the best-fit ellipse. For Ideal polygon columnar joint, r is equal to 1. This means

the columnar joint is completely isometry. In fact, r is not equal to 1 and the columnar joint is anisometry.

Maturation of columnar joint can be determined from

1) Hexagonal index; for high maturity the hexagonal index tends to 0.
2) Mean axial ratio; for high maturity the average axial ratio tends to 1.
3) Average number of side; for high maturity average number of side tends to 6

2.7 Rock classification

Chemical classification schemes are vary according to chemical component and analytical method. With the advance of XRF analysis, rock can be classified on the basis of their major composition and mineralogical criteria.

By using Silica content, the rock can be simply classified into 4 categories as follow.

1st group: felsic igneous rocks containing a high silica content, greater than 63% SiO_2

2nd group: intermediate igneous rocks containing between 52 – 63% SiO_2

3rd group: mafic igneous rocks have 45 – 52% SiO_2 and typically high iron and magnesium content

4th group: ultramafic rock igneous rocks with less than 45% SiO_2

2.7.1 The total alkalis-silica diagram

Author uses the oxide-oxide plots due to the XRF-analysis of columnar rock in the study area. This oxide-oxide major element plots are the most suitable method to classify volcanic rock. The total alkalis-silica diagram (TAS) is the most useful diagram for volcanic rock by using the sum ofNa_2O+K_2O content and the SiO_2 content as wt% oxides to plot onto the diagram in figure.13.

The TAS diagram, showing in figure 13, divides rocks into ultrabasic, basic, intermediate, and acid. This diagram is suitable for the common fresh volcanic rock. But, it is not appropriate to K-rich and Mg-rich rock and also not suitable to weathered, altered, and metamorphose volcanic rock. Since the alkaline minerals are mobilized by those processes. TAS diagram is also used to discriminate alkaline and sub-alkaline rock series.

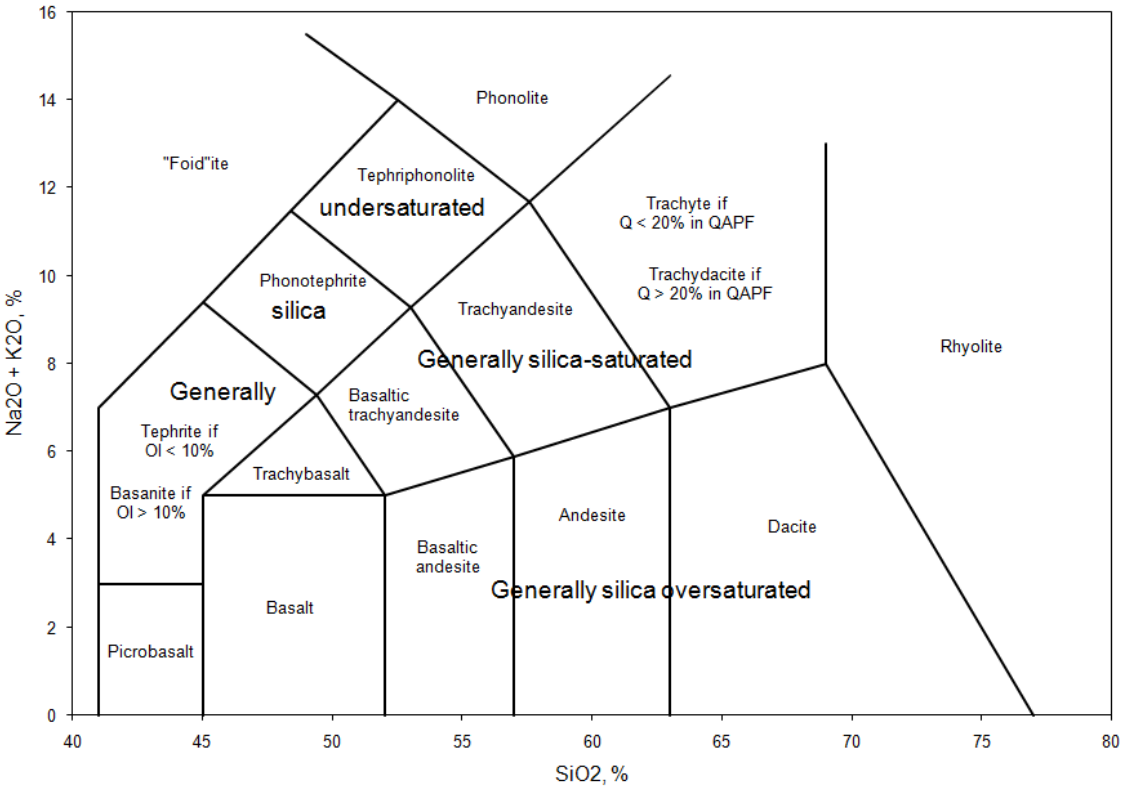

Figure. 13 Plot of SiO_2 vs. Na_2O+K_2O for volcanic rocks (LeBas et al., 1986)

2.7.2 Alkaline/Subalkaline Rocks

There is one of the general classification schemes which divide rocks into alkaline and subalkaline. This criterion is based solely on alkali content (Na_2O+K_2O) vs. silica content as shown in figure 14.

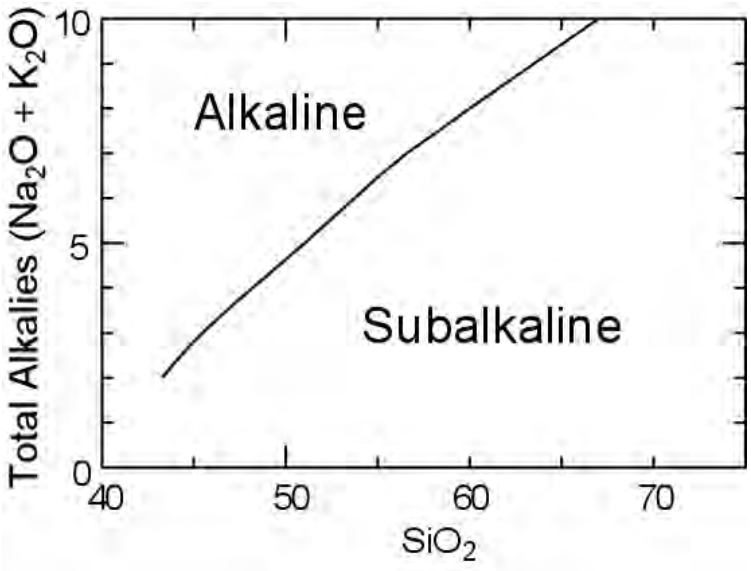

Figure. 14 The plot of alkali content vs. silica content which divides rocks into alkaline and subalkaline (from: www.tulane.edu/~sanelson/eens212/igrockclassif.htm)

However, volcanic rocks of subalkaline series can be further classified into low-K, medium-K, and high-K type by using the K_2O vs SiO_2 diagram as shown in figure 15.

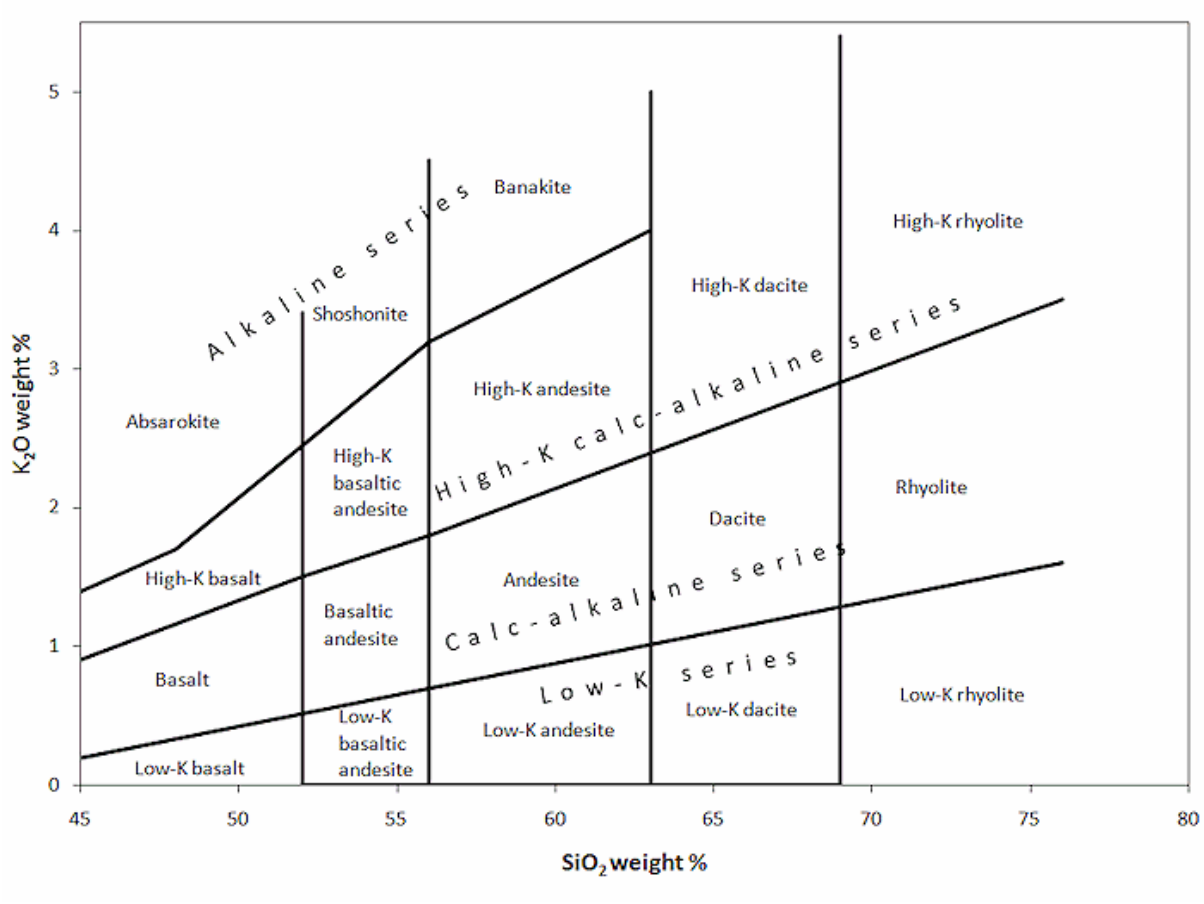

Figure. 15 The plot of SiO_2 vs. K_2O for volcanic rocks (Ewart, 1982)
(From: minerva.union.edu/hollochk/c_petrology/discrim.html)

2.7.3 Classifying igneous rocks using the norm

The norm calculation is a way of the mineralogy forming a rock by chemical analysis.

Alumina (Al_2O_3) Saturation

1) Peraluminous is the rock that has aluminar more than minerals which formed feldspar: $Al_2O_3 > (CaO + Na_2O + K_2O)$
An Al_2O_3-rich mineral present as a common mineral - such as muscovite, corundum, and topaz.

2) Metaluminous is the rock that is composed of the molecular percentages as follows: $Al_2O_3 < (CaO + Na_2O + K_2O)$ and $Al_2O_3 > (Na_2O + K_2O)$ This kind of rock is lack of an Al_2O_3-rich mineral and lack of sodic pyroxenes and amphiboles.

3) Peralkaline rocks are oversaturated with alkalies ($Na_2O + K_2O$), and undersaturated with Al_2O_3. $Al_2O_3 < (Na_2O + K_2O)$

2.7.4 CIPW norm calculation

CIPW norm calculation is used to idealize component of igneous rock by using bulk chemical analysis. Norm is usually used for classification or comparison purpose in fine-grain volcanic rock. The normative „minerals" are calculated to present the possible minerals that might crystallize if the rock were cooled under perfect conditions.

In order to calculate CIPW norm the author uses Excel spreadsheet program written by Kurt Hollocher, Geology Department, Union College, Schenectady, New York. X-ray fluorescence (XRF) is used to analyze the oxide element of bulk rock data and collected the data to apply in CIPW norm calculation.

Unit 3

Method

As the purpose of this project is to study the characteristics of columnar joints, the methodology of this project need to set in order to process the project neatly. After, reviewing many literatuers of relative research, the methodology is revised to be the most fit with this project as follow.

3.1 Review previous studies and research the method of pervious research, compile all information which is relate to the geological data in the project.

3.2 Go field trip and collect geometry of columnar basalt by taking picture perpendicular to the upper surface of columnar joint and measure the inclination of columnar basalts. Collect a hand sample in each study area.

3.3 Collect data from field note and pictures by

3.3.1Counting type of fracture intersection

Pollard and Aydin (1988) categorized fracture intersection into three types:

1) T-intersection is T-shape fracture intersection
2) Y-intersection is Y-shape fracture intersection
3) X-intersection is X-shape fracture intersection

Each type is shown in figure 16.

a b c

Figure.16 Three types of fractures intersection. (a) is T-intersection, (b) is Y-intersection, (c) is X-intersection.

3.3.2 Counting the number of side of column. There are 3-8 side of polygon as shown in figure 17.

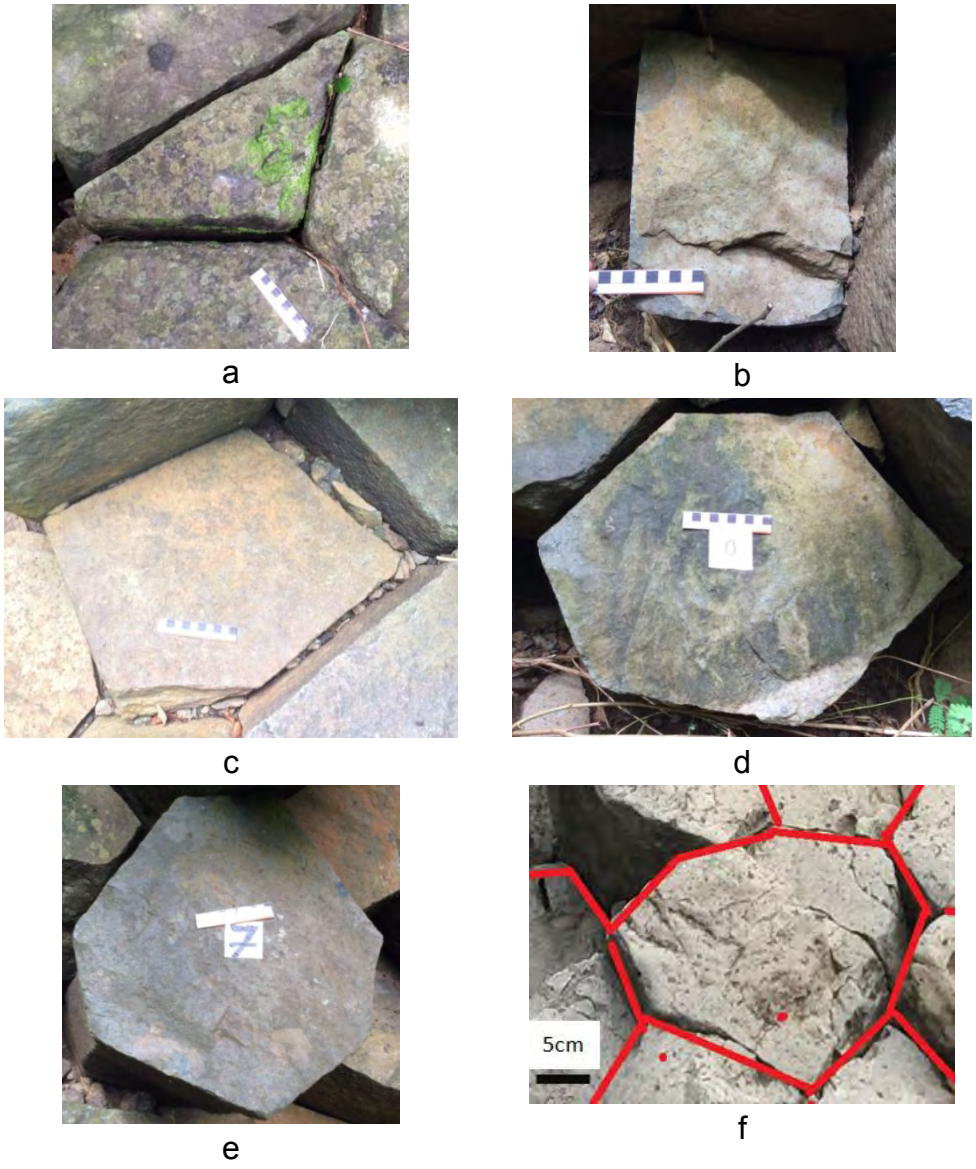

Figure 17 Illustrate 3-8 side polygon. (a) is 3-side polygon, (b) is 4-side polygon, (c) is 5-side polygon, (d) is 6-side polygon, (e) is 7-side polygon, (f) is 8-side polygon

3.3.3 Measuring the longest and shortest axis of the best-fit ellipse in the polygonal shape of uppermost surface of column as shown in figure 18.

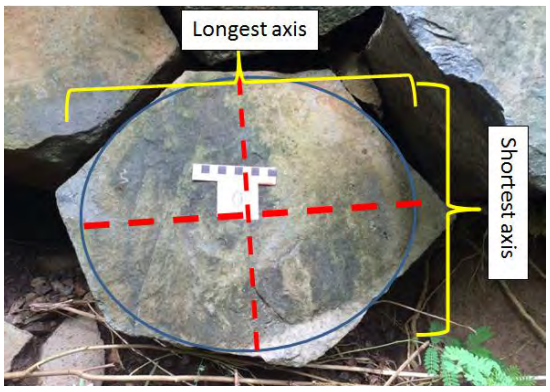

Figure. 18 The best-fit ellipse that fit in polygon with longest axis and shortest axis.

3.3.4 The length of longest axis and shortest axis of each polygon.

3.4 Calculate

3.4.1 hexagonality index: $X_N=(f_5+f_7+4(f_4+f_8)+9f_3)^{1/2}$

3.4.2 average side number: $n = 2(2J_T+3J_Y+4J_X)/(J_T+J_Y+2J_X)$

3.4.3 Axial ratio: r=a/b

3.4.4 Average diameter. Largest axis of polygon and shortest axis of polygon divided by two

3.5 Analyze hand specimen by using X-Ray Fluorescence analysis and prepare rock thin section for inspecting texture of rock by light microscope.

Note that: the process of XRF analysis is analyzed at Geology department faculty of Science, Chulalongkorn University. The details of X-Ray Fluorescence Spectrometer is shown below.

Analytical Instrument:	X-Ray Fluorescence Spectrometer (XRF) : Bruker AXS, Germany Model: S4 Pioneer Wavelength dispersive X-Ray Fluorescence (WDXRF) Spectrometry
Voltage/Current:	60 kV / 50 mA
Conditions:	Range 0.2 – 20 A (60 – 0.6 keV) Total resolution 3 – 100 eV Typical measurement time 2 – 10 s per element
Program used:	SPECTRA Plus software of the Bruker with the standardless Analysis.

3.6 Calculate CIPW Norm by using Excel spreadsheet program written by Kurt Hollocher, Geology Department, Union College, Schenectady, New York. Plot the graph of mineral composition in order to classify rock type and descript rock texture under light microscope.

3.7 Correlate the relationship between each variant including hexagonality index, Axial ratio, average side number, and average diameter to infer the character of columnar basalt.

3.8 Submit the report and Present the project.

Unit 4

Result

4.1 Columnar characteristic

4.1.1Study Area 1: Sao-Hin Donsawan House of priest, Tumbon Khok Prong Amphoe Wichian Buri, Changwat Phetchabun

This area is channel, natural outcrop, 20 meters long and 4 meter high.

This area is shown in figure 19.

Figure 19 Character of columnar basalt at Sao-Hin Donsawan

Descriptive: Columnar basalts in this area are black color and slightly weathering. Some columns are tilted at different angle. In the channel, columnar basalt is perpendicular to the ground surface; whereas, columnar basalt near the river bank inclines (The column tilted to North direction with inclination angle is vary 20-60). The average diameter of the columns is about 40 cm. The height of the columns expose above the ground surface about 4 meters. The fractures are well developing, quite straight, and fracture spacing is about 3mm-15mm, 5 mm in average. No undulation of column width.

Rock details (Observed by hand lens): Fresh color is black; whereas, weathered color is grayish-brown. There is porosity around the outer surface of some column. There are euhedral phenocrysts, lath shape mineral, which its size is 5-10 mm, in Aphenitic texture.

1)The number of n-side polygons

3-side polygon: 6 columns

4-side polygon: 31 columns

5-side polygon: 128 columns

6-side polygon: 105 columns

7-side polygon: 15 columns

8-side polygon: 0 columns

There are 3 to 7 sides of polygon for the total of 285 columns in this area.

Then calculate the hexagonality index : $X_N=(f_5+f_7+4(f_4+f_8)+9f_3)^{1/2}$

Where f_n is the function of n-side polygon.

Yield X_N= 1.06

2)The number of Type-intersection

T- intersections: 44 intersections

X- intersections: 73 intersections

Y- intersections: 273 intersections

Then calculate the average side number: $n = 2(2J_T+3J_Y+4J_X)/(J_T+J_Y+2J_X)$

where J_T =A number of T- intersection/ total ofintersecton,
J_Y =A number of Y- intersection/ total of intersectons,
J_x =A number of X- intersection/total of intersectons.

Yield n= 5.18

3)The average diameter of polygon

The major axis ranges between 25.92 cm to 94.25 cm and the average major axis is 47.31 cm

The minor axis ranges between 15.8cm to 75.47 cm and the average minor axis is 33.70

By average the major axis and minor axis of the polygonal face across the columnar, the average diameter is 40.59 cm.

4)The axial ratio

By measuring the longest and shortest axis of the best-fit ellipse in the polygonal shape of uppermost surface of column, calculate the axial ratio by:

Axial ratio r=a/b
where a is major diameter of the best-fit ellipse
b is minor diameter of the best-fit ellipse
Yield minimum r is 1 and maximum r is 2.64

Average axial ration: r = 1.45

Note that: The average diameter and axial ratio are measured form 143 columns which are perpendicular to the photo direction. If the column is not perpendicular to the photo, the length measured in the picture might not correct due to the contraction or dilation of the picture.

5) The result from X-Ray Fluorescence(XRF)

Table 3. Result from X-Ray Fluorescence analysis of rock at Sao-Hin Donsawan

Formula	Z	Concentration(%wt)	XRF %
SiO_2	14	45.70	45.7
Al_2O_3	13	18.40	18.37
CaO	20	9.90	9.904
Fe_2O_3	26	9.90	9.901
Na_2O	11	4.99	4.986
MgO	12	4.95	4.946
TiO_2	22	1.92	1.92
P_2O_5	15	1.37	1.37
K_2O	19	1.34	1.34
SrO	38	0.22	0.2178
MnO	25	0.17	0.17
LOI		1.01	
	total	99.87	

6) CIPW Norm calculation using data from XRF analysis

Table 4. Result of CIPW Norm calculation of rock at Sao-Hin Donsawan

Normative Minerals	Weight % Norm	Volume % Norm
Plagioclase	52.97	58.47
Orthoclase	7.92	9.15
Nepheline	7.10	8.21
Diopside	8.56	7.87
Olivine	5.86	5.39
Ilmenite	0.36	0.23
Hematite	9.90	5.58
Apatite	3.17	2.94
Perovskite	2.94	2.18
Total	98.78	100.02

7) Rock texture under light microscope

The rock texture under light microscope reveals the Holocrystalline texture which composes of all crystal of mineral with no glass texture. In more details, it is Aphenitic texture that is cannot observe by eyes. However, observing the texture under light microscope reveals the porphyry textures with average crystals size 0.5 mm-5mm of phenocryst, and the average crystal size of groundmass less than 1 mm. The mineral composition composes of feldspar 50%, opaque mineral 25%, Olivine 10%, Pyroxene 10%, and others 5%.

In more description of composition, Groundmass composes of 35% Plagioclase- acicular (long-slender shape), twin, euhearal, very small (<0.1mm); 25% opaque mineral- very small size(< 0.1 mm); 5% Olivine sub-euhearal, small 0.1-0.3mm; 5% Pyroxene anhedral, small 0.1-0.3mm; 5% others euhedral, brown -isometric mineral. Phenocryst composed of 15% plagioclase size 0.5-2mm; 5% pyroxene size 1-2mm; 5% olivine 1-2mm size.

Special texture features are pyroxene growth in plagioclase crystals, reaction rim of phenocryst, twin in plagioclase, corroded feldspar, xenolith of mafic mineral as shown in figure 20 and figure 21.

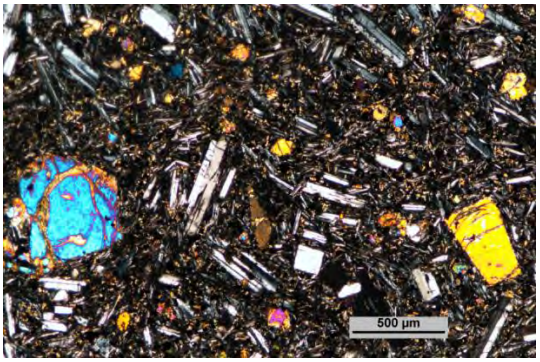

Figure. 20 Columnar basalt texture at Sao-Hin Donsawan

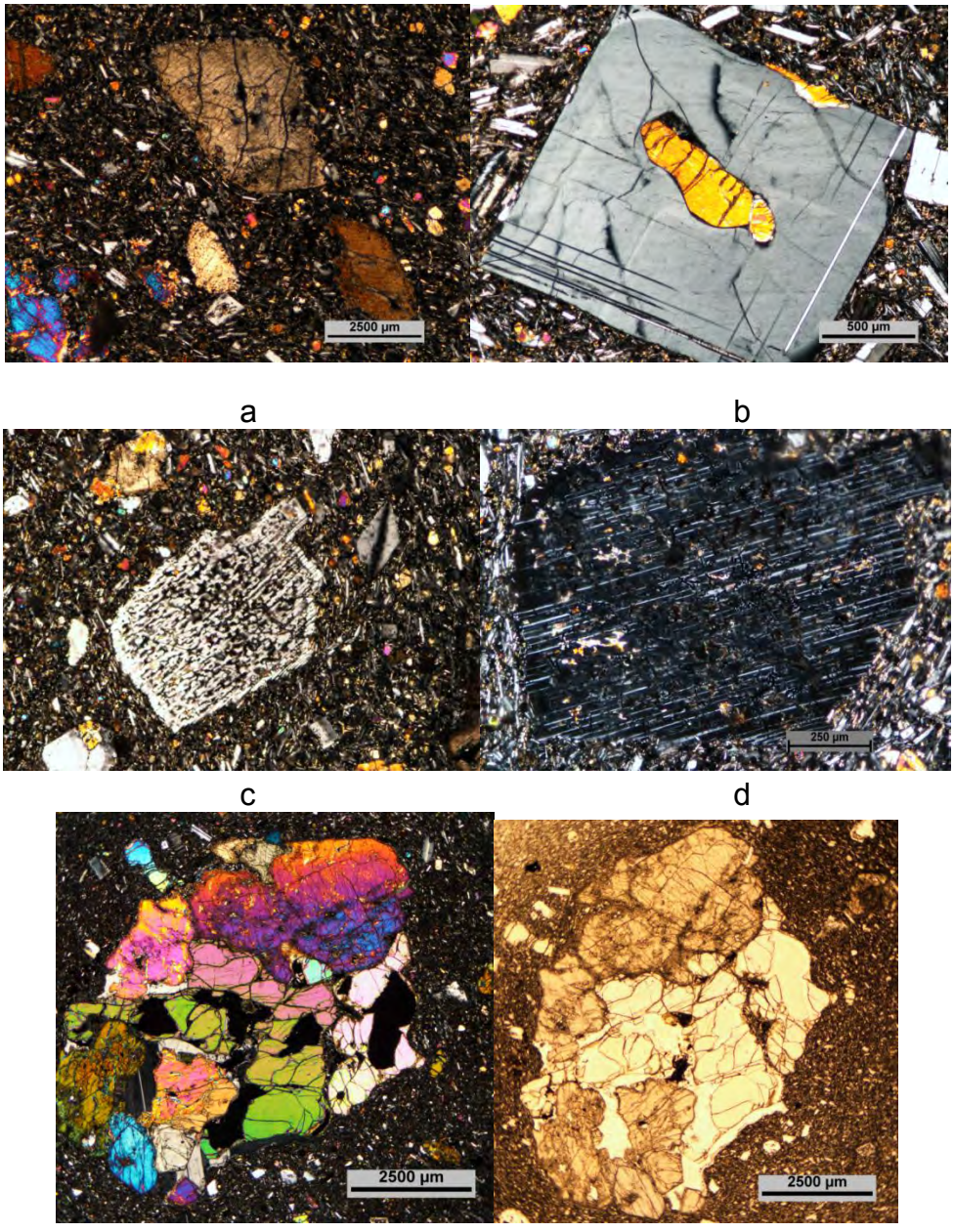

Figure. 21 Some characters of mineral. (a) shows pyroxene crystal, (b) shows pyroxene in plagioclase crystal, (c) and (d) are corroded feldspar, (e) and (f) are mafic- composition xenolith.

4.1.2 Study Area 2: Sub-Phlu waterfall Tumbon Yang Sao, Amphoe Wichian Buri, Changwat Phetchabun

This is natural outcrop, waterfall, 10 meters long and 4 meter high.

This area is shown in figure 22.

Figure. 22 Character of columnar basalt at Sub-Phlu waterfall.

Descriptive: Columnar basalts in this area are black color and slightly weathering. Some columns are tilted at same angle (The column tilted to North direction and dip angle is about 70) as shown in figure 24. The fractures are quit poorly developing, some are curve, and some are unclear. Fracture spacing is about 1mm-2mm. The average size of diameter column is about 30 cm. The columns expose above the ground surface about 4-6 meters. There is little undulation of the column width in some part of the area as shown in figure 23.

Rock details: Fresh color is grayish black; whereas, weathered color is grayish-brown. There is porosity around the outer surface of some columns. There are subhedral phenocrysts which its size is 2-5 mm in Aphenitic texture.

Figure. 23 Undulation of the column width. The column is shown wavy column.

Figure. 24 Column tilted at same angle

1) The number of n-side polygons of the columnar basalts:

3-side polygon: 21 columns

4-side polygon: 87 columns

5-side polygon: 187 columns

6-side polygon: 114 columns

7-side polygon: 23 columns

8-side polygon: 7 columns

There are 3 to 8 sides of polygon for the total of 439 columns in this area.

Then calculate to the hexagonality index: $X_N=(f_5+f_7+4(f_4+f_8)+9f_3)^{1/2}$

Where f_n is the function of n-side polygon.

Yield X_N= 1.33

2) The number of Type- intersections

T- intersection: 180 intersections

X- intersection: 143 intersections

Y- intersection: 405 intersections

Then calculate the average side number: $n = 2(2J_T+3J_Y+4J_X)/(J_T+J_Y+2J_X)$

where J_T =A number of T- intersection/ total ofintersecton
J_Y =A number of Y- intersection/ total of intersectons
J_x =A number of X- intersection/ total of intersectons

Yield n= 4.93

3) The average diameter of polygon

The major axis ranges between 14.92cm to 58.55cm and the average major axis is 36.36 cm.

The minor axis ranges between 12.74cm to 50.43cm and the average minor axis is 26.24cm.

By average the longest axis and shortest axis of the polygonal face across the columnar, the average diameter is 31.30 cm.

4) The axial ratio

By measuring the longest and shortest axis of the best-fit ellipse in the polygonal shape of uppermost surface of column, calculate the axial ratio by:

Axial ratio r=a/b

where a is major diameter of the best-fit ellipse
b is minor diameter of the best-fit ellipse
Yield minimum r is 1 and maximum r is 2.96

Average axial ratio: r= 1.42

Note that: The average diameter and axial ratio are measured form 176 columns which are perpendicular to the photo direction. If the column is not perpendicular to the photo, the length measured in the picture might not correct due to the contraction or dilation of the picture.

5) The result from X-Ray Fluorescence(XRF)

Table 5. Result from X-Ray Fluorescence analysis of rock at Sub-Phlu waterfall

Formula	Z	Concentration(%wt)	XRF %
SiO_2	14	45.30	45.28
Al_2O_3	13	16.70	16.73
Fe_2O_3	26	11.80	11.83
CaO	20	10.00	10.03
MgO	12	6.63	6.627
Na_2O	11	3.16	3.16
TiO_2	22	2.36	2.36
K_2O	19	2.01	2.01
P_2O_5	15	0.60	0.596
MnO	25	0.17	0.165
SrO	38	0.11	0.107
LOI		0.90	
Total		99.73	

6) Norm calculation using data from XRF analysis

Table 6. CIPW Norm calculation of rock at Sub-Phlu waterfall

Normative Minerals	Weight % Norm	Volume % Norm
Plagioclase	50.15	56.30
Orthoclase	11.88	14.01
Nepheline	1.10	1.30
Diopside	10.15	9.52
Olivine	8.27	7.76
Ilmenite	0.36	0.23
Hematite	11.80	6.79
Apatite	1.39	1.31
Perovskite	3.69	2.79
Total	98.79	100.01

7) Rock Texture under light microscope

The rock texture under light microscope reveals the Holocrystalline texture which composes of all crystal of mineral with no glass texture. In more details, it is Aphenitic texture that is cannot observe by eyes. However, observing the texture under light microscope reveals the porphyry textures with average crystals size 2mm-3mm of phenocryst, and the average crystal size of groundmass less than 1 mm. The mineral composition composes of feldspar 50%, opaque mineral 25%, Olivine 10%, Pyroxene 15%.

In more description of composition, Groundmass composes of 35% Plagioclase- acicular (long-slender shape), twin, euhearal, very small (<0.1mm); 25% opaque mineral- very small size(< 0.1 mm); 5% Olivine sub-euhearal, small 0.1-0.3mm; 5% Pyroxene anhedral, small 0.1-0.3mm. Phenocryst composed of 15% plagioclase size 0.5-2mm; 10% pyroxene size 1-2mm; 5% olivine 1-2mm size.

Special texture features are pyroxene growth in plagioclase crystals, reaction rim of phenocryst, twin in plagioclase, corroded feldspar, xenolith of mafic minerals as shown in figure 25 and figure 26.

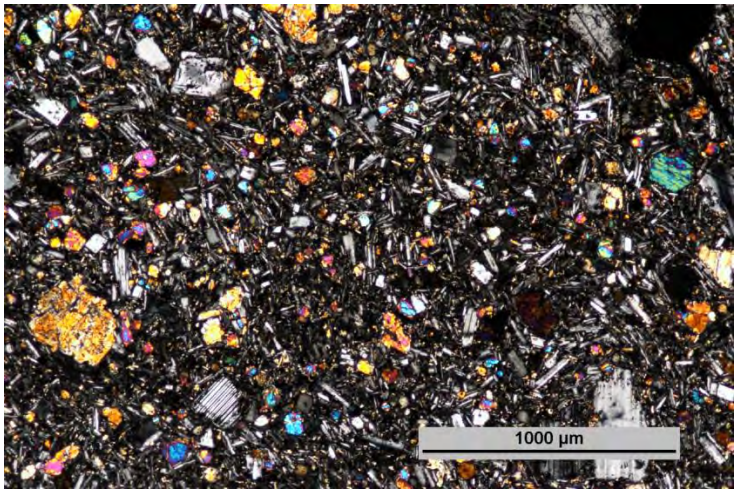

Figure. 25 Columnar basalt texture at Sub-Phlu waterfall

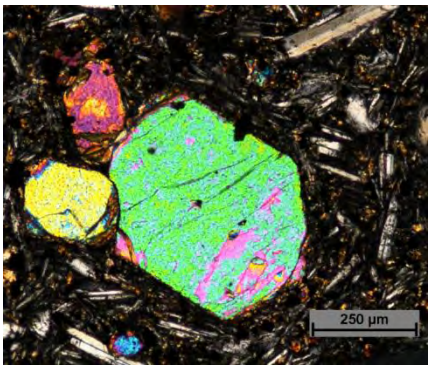

(a)

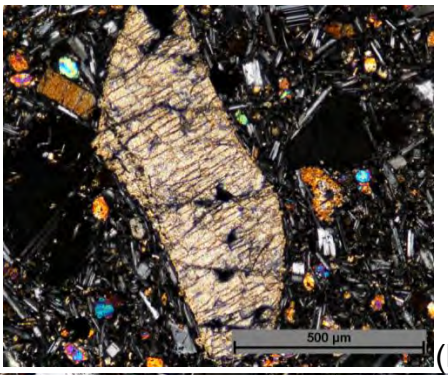

(b)

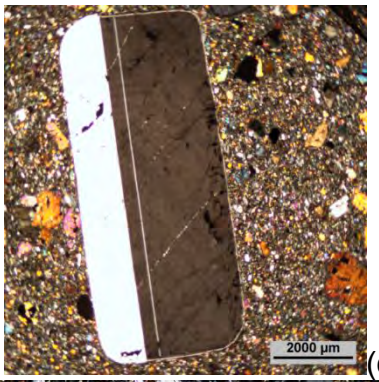

(c)

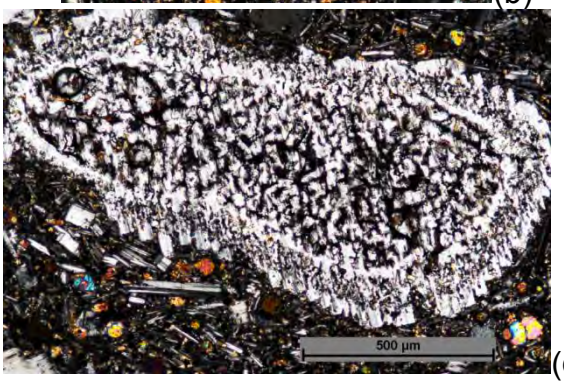

(d)

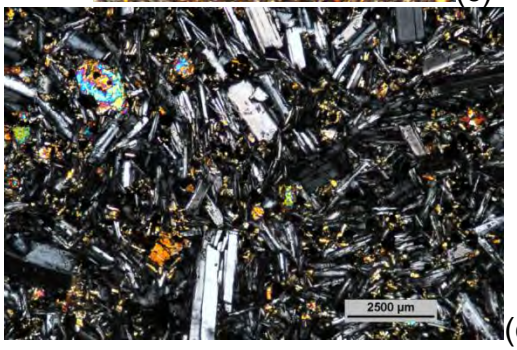

(e)

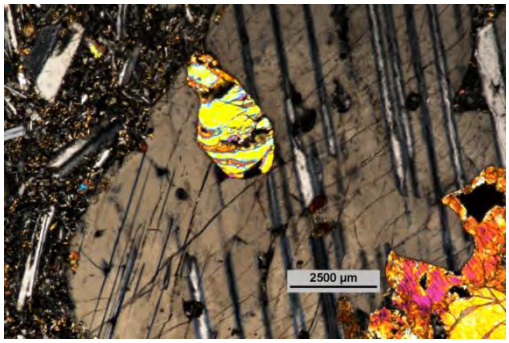

(f)

Figure. 26 Some characters of mineral. a shows olivine crystal, b shows pyroxene crystal, c shows plagioclase crystal, d is corroded feldspar, e shows the lath shape euhedral of plagioclase, and f olivine crystal in plagioclase crystal

Unit 5

Discussion

5.1 Columnar joint characteristics

Compare raw data of the n-side columnar basalt in Sao-Hin Donsawan and Sub Phlu waterfall

Table 7. The number of n-side columnar basalt in two study areas

n-side	Sao-Hin Donsawan	Sub Phlu
3	6	21
4	31	87
5	128	187
6	105	114
7	15	23
8	0	7
total	285	439

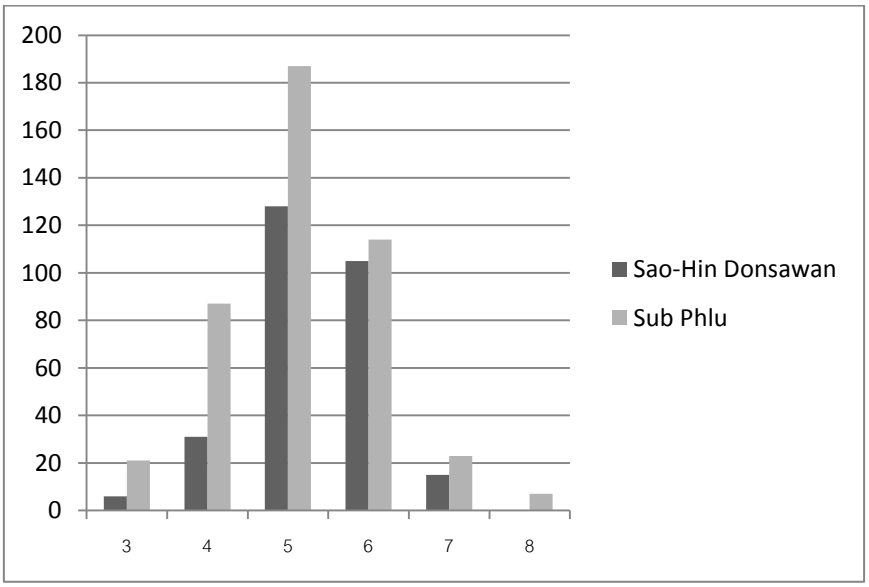

Figure. 27 Graph shows the number of n-side columnar basalt in two study areas

As showing in graph and table in Tabel 7 and Figure 27, pentagonal and hexagonal columnar basalt are predominant in both areas. The trend of the number of columnar in each n-side polygon is look similar to bell shape. However this data

are not directly comparable. Because the total number of columnar in both area is not the same, these data are calculated into percentage.

Calculate n-side column into 100 percent in each area.

Table 8. Percentage of n-side column in two study areas

n-side	Sao-Hin Donsawan (%)	Sub-Phlu(%)
3	2.11	4.29
4	10.88	14.29
5	44.91	44.29
6	36.84	28.57
7	5.26	7.14
8	0	1.43

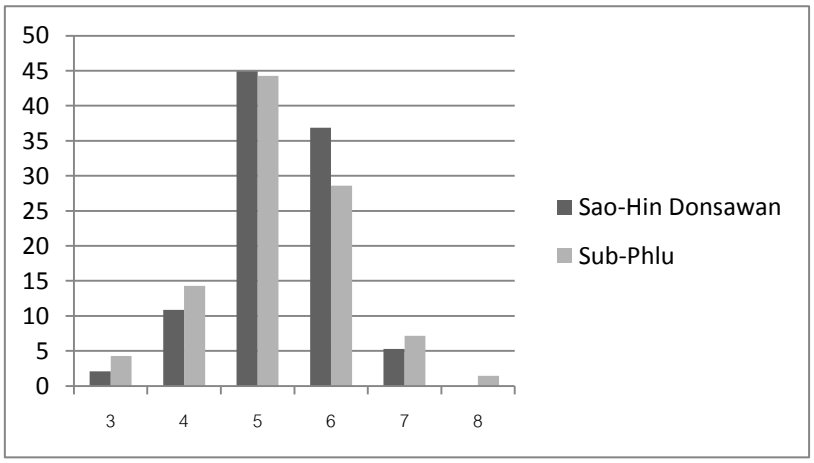

Figure. 28 Graph shows the percentage of n-side column in two study areas

The graph shows the percentage of n-side polygonal column in Sao-Hindonsawan and Sub-Phlu waterfall (Table 8 and Figure 28). The majority is pentagonal column which nearly accounts to 45% in both areas. The Second is hexagonal column, being responsible for 36.84% and 28.57% in Sao-Hindonsawan and Sub-Phlu waterfall respectively. The number of hexagonal and pentagonal column in Sao-Hindonsawan is greater than that in Sub-Phlu waterfall. Moreover, the number of 3,4,7, and 8- side polygonal column in Sub-Phlu waterfall is greater than that in Sao-Hindonsawan. Since the mature columnar basalt tends to be pentagonal and hexagonal pattern, and the 3, 4, 7, and 8-side polygon are less in the mature one. The number of hexagon and pentagon is greater in Sao-Hindonsawan. And the number of 3, 4, 7, and 8-side polygon are clearly less than those in Sao-Hindonsawan. These numbers imply that the columnar basalt in Sao-Hindonsawan is more mature than column in Sub-phlu waterfall.

Compare type of intersection by calculating the data into percentage.

Table 9. Percentage of intersection types of columnar joint

Intersection type	Sao-Hin Donsawan	Sub Phlu
T	11.28	24.73
x	18.72	19.64
y	70	49.3

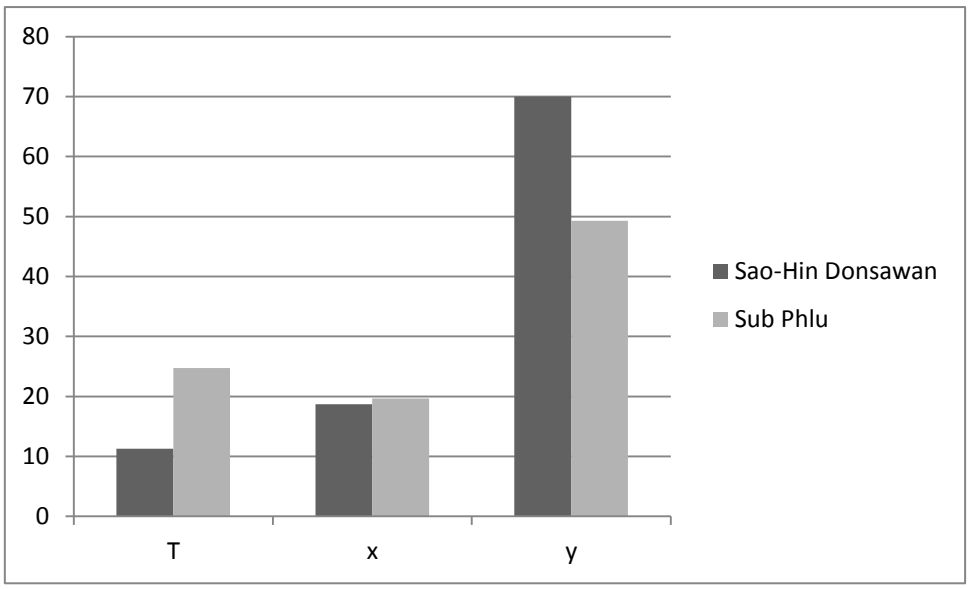

Figure. 29 Graph shows the percentage of intersection types of columnar joint

The graph shows the percentage of intersection type in Sao-Hindonsawan and Sub-Phlu waterfall (Table 9 and Figure 29). The majority is Y-intersection in both areas. The number of Y-intersection at Sao-Hindonsawan is up to 70% which is more than that in Sub-Phlu waterfall, accounting to 50%. The number of X-intersection in both areas is nearly the same. But, the number T-intersection in Sub-Phlu waterfall is significantly greater than another. In immature crack pattern, the X-type crack and T-type crack is predominant, whereas Y-type junction is found in mature crack pattern. So, the mature columnar basalt tends to have more y-intersection and less in T and X-intersection. The number of Y-intersection is extremely greater in Sao-Hindonsawan. And T and X-intersection are clearly less in Hindonsawan. These numbers imply that the columnar basalt in Sao-Hindonsawan has high maturity.

The average diameter of polygon in Sao-Hin Donsawan, the average diameter is 40.59 cm. The other length details are shown in the Table 10.

Table 10.Aaverage diameter of columnar basalt at Sao-Hin Donsawan

	minimum	Maximum	average	deviation
Major axis	25.92	94.25	47.31	11.18
Minor axis	18.5	75.47	33.70	9.43

The average diameter of polygon in Sub-Phlu waterfall, the average diameter is 31.30 cm. The other length details are shown in the Table 11.

Table 11. Average diameter of columnar basalt at Sub-Phlu waterfall

	minimum	maximum	average	deviation
Major axis	14.92	58.55	36.36	8.34
Minor axis	12.74	50.43	26.24	7.08

As seen in the tables of diameter data, the diameter of polygon in Sao-Hin Donsawan is bigger than that in Sub-Phlu waterfall. The length of major and minor axis in Sao-Hin Donsawan is significantly longer than those in Sub-Phlu waterfall. The cooling rate controls size of column. It is inversely to the function of column size. The bigger polygon implies the slow cooling rates. Columnar basalts at Sao-Hin Donsawan may has slower cooling rate comparing to those in Sub-Phlu waterfall. Rapid evolution of crack in cooling lava yields equal size of column. Hence, the deviation of column diameter at Sub-Phlu waterfall is not high. However, the larger deviation of the measured length in Sao-Hin Donswan may be resulted from the non-homogeneous of basalt composition because the rock uniformly cracks if the composition of the molten rock is homogeneous.

Table 12. Average number of side, Hexagonality index, and Axial ratio

	Average number of side	Hexagonality	Axial ratio
Sao-Hin Donsawan	5.18	1.06	1.45
Sub-Phlu waterfall	4.93	1.33	1.42

5.1.1 Average number of side

It is believed that if T-type intersection is dominant, in imature crack, n-number is approximately 4. The Y-type intersection is dominant in mature crack pattern, the n-number is nearly 6. From the Table 12, the average number of side at Sao-Hin Donsawan is 5.18 which is greater than a the number at Sub-Phlu waterfall, 4.93. Then the columnar basalt at Sao-Hin Donsawan has higher maturity than basalt at Sub-Phlu waterfall.

5.1.2 Hexagonality Index

As the ideal columnar joint growth and mature, low number-side polygons turn to be six sides polygons and Hexagonality index tends to 0. This means that the lower hexagonality index, the more maturity of the columnar joint will be.The hexagonality index at Sao-Hin Donsawan is 1.06 whereas the index at Sub-Phlu waterfall is 1.33. The index at Sao-Hin Donsawan is lower, then the maturity of columnar joint at this area is better.

5.1.3 Axial ratio

For Ideal polygon columnar joint, r is equal to 1. This means the columnar joint is completely isometry. In fact, r is not equal to 1 due to some of inhomogeneous of lava masses. The axial ratio at Sao-Hin Donsawan and Sub-Phlu waterfall is 1.45and 1.42 respectively. So, that this implies that the columnar basalt in Sub-Phlu waterfall is more mature, however the difference of axial ratio may be influence by the inhomigeneous of basalt rock. The difference of the value is slightly different, only 0.03. Thus, the columnar basalts in these two areas are unclearly distinguished by using axial ratio.

5.2 Basalt Classification

Table 13. Chemical component by XRF analysis of columnar basalt in two study areas

Formula	Sao-Hin Donsawan Concentration(%wt)	Sub-Phlu waterfall concentration(% wt)
SiO_2	45.7	45.3
Al_2O_3	18.4	16.7
CaO	9.9	10
Fe_2O_3	9.9	11.8
Na_2O	4.99	3.16
MgO	4.95	6.63
TiO_2	1.92	2.36
P_2O_5	1.37	0.6
K_2O	1.34	2.01
SrO	0.22	0.11
MnO	0.17	0.17
LOI	1.01	0.89
Total	99.87	99.73

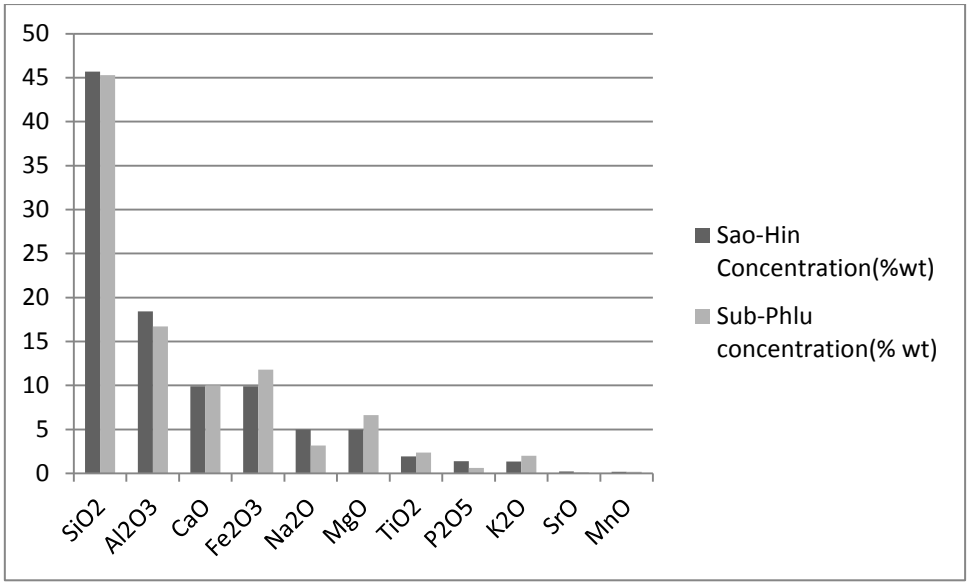

Figure. 30 Graph shows chemical component by XRF analysis of columnar basalt in two study areas

As seen from the graph in Table 13 and Figure 30, the chemical composition is nearly the same. The silica content in both rocks is 45% which can be classified into mafic igneous rock. Both of chemical rock compositions containing molar(K_2O + Na_2O)/ Al_2O_3 are 0.3 (below 1) can be group into Peraluminous. The content of Fe and Mg in the rock at Sub-Phlu is higher than that in Sao-Hin Donsawan. Over all, most of mineral content is nearly similar to each other. So, the rock classification might not a big different.

Table 14. Norm calculation by using XRF-data of columnar basalt in two study areas

Normative Minerals	Weight % Sao-Hin	Weight % Sub-Phlu
Plagioclase	52.97	50.15
Orthoclase	7.92	11.88
Nepheline	7.1	1.1
Diopside	8.56	10.15
Olivine	5.86	8.27
Ilmenite	0.36	0.36
Hematite	9.9	11.8
Apatite	3.17	1.39
Perovskite	2.94	3.69
Total	98.78	98.79

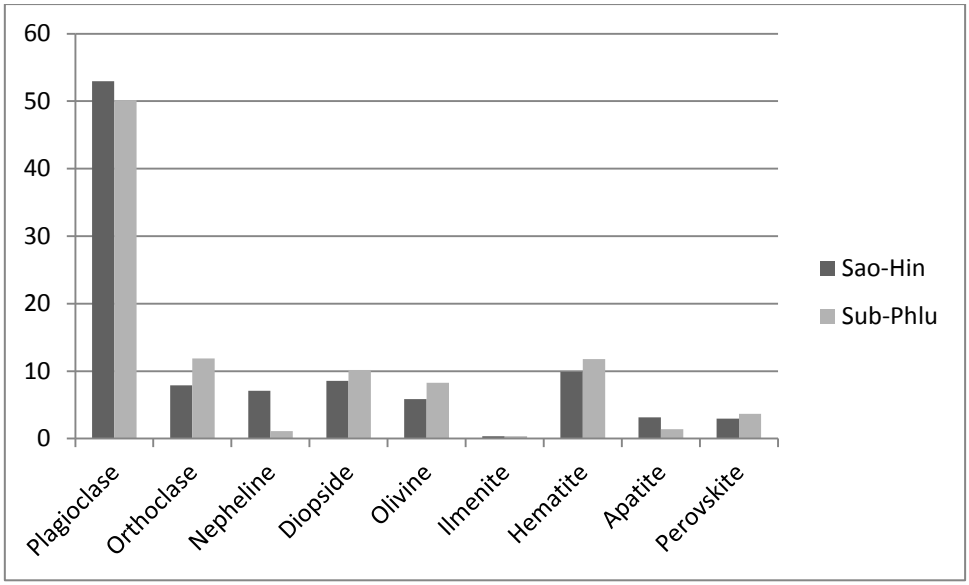

Figure. 31 Graph shows Norm calculation by using XRF-data of columnar basalt in two study areas

To compare ideal mineral forming rock, Norm is used to calculate the mineral assemblage as a model. As seen from the graph in Table 14 and Figure 31, plagioclase is dominant up to 50%. Other minerals including olivine, pyroxene, hematite, nepheline, apatite, perovskite are lower than 10%. There are a little different between two samples. The rock at Sao-Hin Donsawan has higher content of plagioclase, nepheline, and apatite whereas the rock at Sub-Phlu waterfall has higher content of orthoclase, olivine, pyroxene, hematite, perovskite. These mean that basalt at Sub-Phlu waterfall has more mafic-mineral content than the rock in Sao-Hin Donsawan.

One of general igneous rock classification is divided rock into two categories; alkaline and subalkaline rock as shown in figure 32.

Basalt from those two study area are classified into alkaline rock.

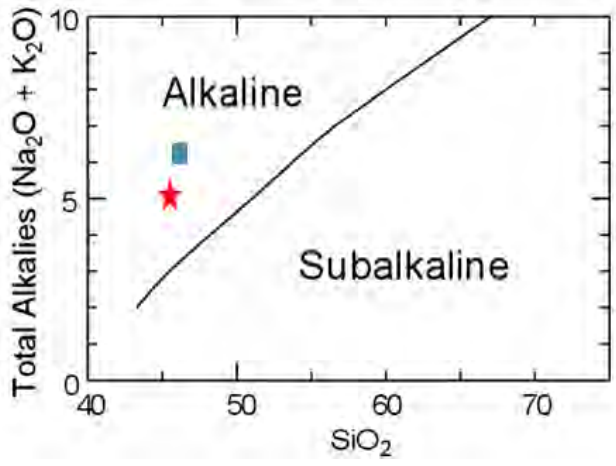

Figure. 32 Plot of SiO_2 vs the total Na_2O+ K_2O of rock composition in the study areas

Basalt at Sao-Hin Donsawan is composed of SiO_2 45.70% wt and Na_2O+K_2O 6.33%wt. Then can be classified into alkaline rock.

Basalt at Sub-Phlu waterfall is composed of SiO_2 45.30% wt and Na_2O+K_2O 5.17%wt. Then can be also classified into alkaline rock.

However, volcanic rocks of subalkaline series can be further classified into low-K, medium-K, and high-K type by using the K_2O vs SiO_2 diagram as shown in figure 33.

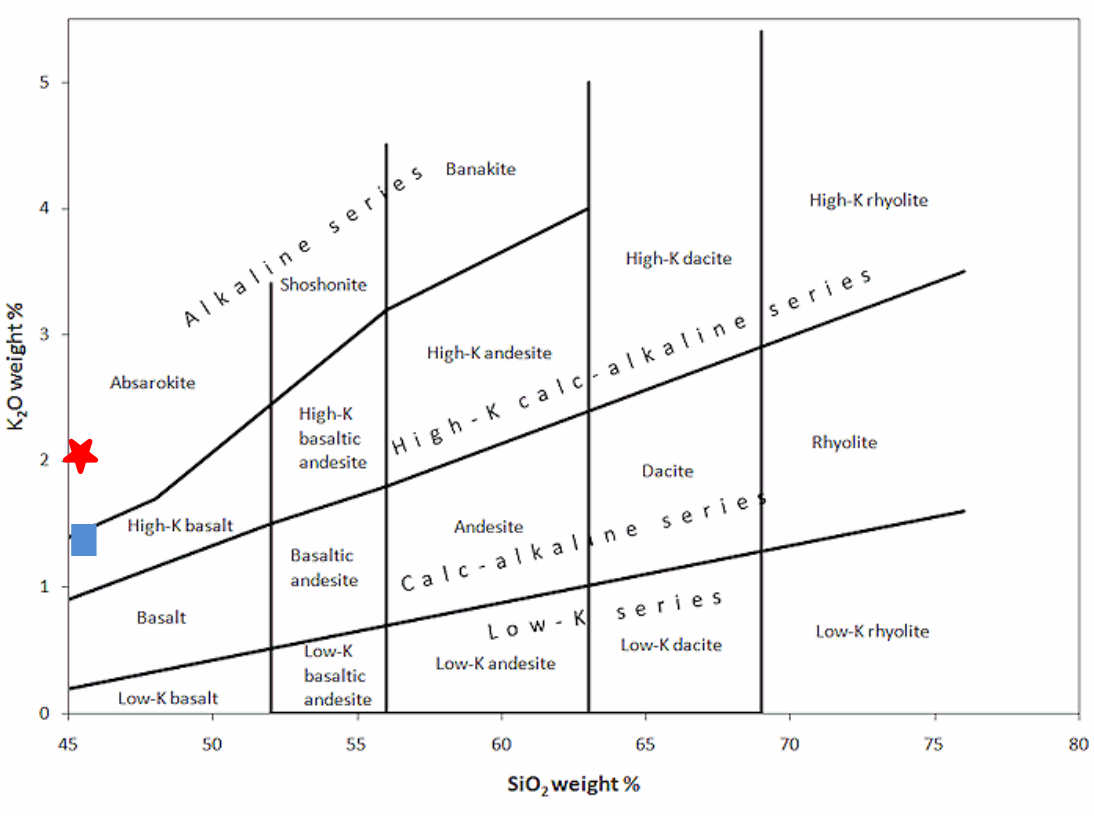

Figure. 33 Plot of of SiO_2 vs K_2O of rock composition in the study areas

Basalt at Sao-Hin Donsawan is composed of SiO_2 45.70% wt and K_2O 1.34%wt which can be classified into absarokite, alkaline Series

Basalt at Sub-Phlu waterfall is composed of SiO_2 45.30% wt and K_2O 2.01%wt which can be classified into high-K basalt, high-K calc- alkaline serie

Chemical classification and nomenclature of volcanic rocks using the total alkali versus silica (TAS) diagram is shown in figure 34.

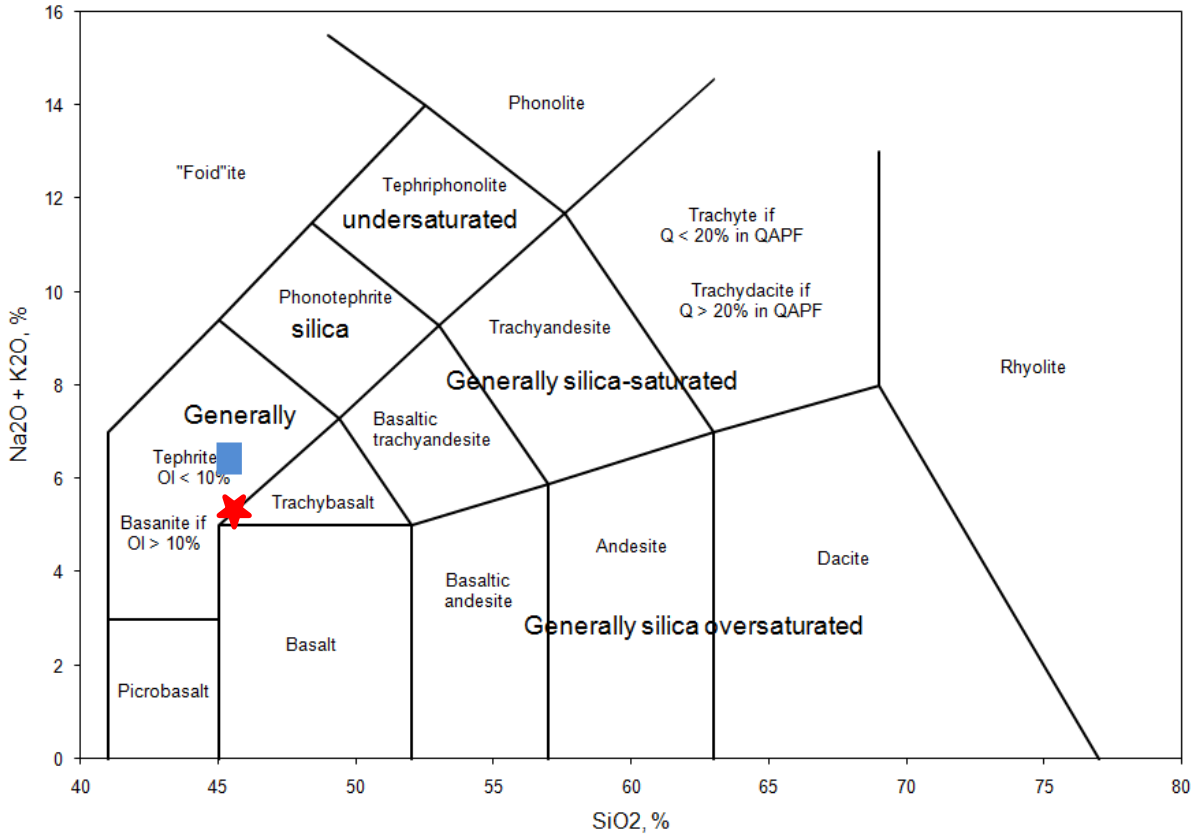

Figure. 34 Plot of the total alkali versus silica of rock composition in the study areas

Basalt at Sao-Hin Donsawan is composed of SiO_2 45.70% wt and Na_2O+K_2O 6.33%wt. Then can be classified into tephrite.

Basalt at Sub-Phlu waterfall is composed of SiO_2 45.30% wt and Na_2O+K_2O 5.17%wt. Then can be classified into tephrite to trachy-basalt.

Both rock at Sao-Hin Donsawan and Sub-Phlu waterfall have holocrystalline texture, average aroundmass is less than 0.1mm. Phenocryst in Sao-Hin Donsawan has wide range of size 0.5-5 mm, whereas phenocryst in Sub-Phlu waterfall ranges 2-3 mm. Main mineral composition of rock is nearly the same which compose of feldspar50%, opaque mineral 25%, olivine 10%, pyroxene 10%-15%. Groundmass is mainly composed of acicular plagioclase and opaque mineral. Plagioclase, olivine, and pyroxene are commonly phenocrysts. Plagioclase- acicular (long-slender shape) with twins is dominant character of plagioclase crystals. There are also growths of pyroxene in plagioclase crystal, reaction rim of plagioclase phenocryst, corroded feldspar, and xenolith of mafic mineral. As all of these textures observed by light microscope, both rocks cannot differentiate since the characteristics of both thing sections are almost similar.

Sobolev et al., (1971) studeid melt inclusions in phenocrysts from nepheline basalt, fergusite porphyry, and tephrite and proposed that clinopyroxene in the range 1380–1250°. Since the basalt composition of both of study areas is tephrite and the phenocryst of the rock sample is nearly the same such as diopside(clinopyroxene) and olivine . The temperature of the magma in both areas may range in between 1380-1250 degree celsius compared with the study.

5.3 The origin of columnar basalt

From previous study (Suttirat et al., 1994) basalt in Amphoe Wichian Buri is Cenozoeic basalt which originates within Cenozoic basins in Thailand. These Cenozoeic basins are developed in Late Eocene to early Oligocene as a result of the extrusion tectonics of Southeast Asian block along the major NE-SW trending fault zones.

There are four main tectonic episodes for major Cenozoic Basin development

The first stage is the pull-apart and initial transtensional synrifting event (55 - 35Ma). This occurs by the continental extension and mantle plume due to the interaction of subduction of India and Asia.

The second stage is the thermal subsidence event (35 - 15 Ma) involving the significant transtensional event with rapidly basinal subsidence. Several basins were occupied by several fresh water lakes and carbon/hydrocarbon accumulation.

The third stage is transpression wrenching event (15 - 10 Ma) with basin inversion, folding, and extensive basin with high volcanism.

The last stage is post-rifting event (10 Ma –Recent). Onshore basins became terrestrial deposits whereas those in the Gulf were gradually subsided with marine incursion.

The age of Basalt in the studies area is in the last stage, post-rifting event. Basaltic rock in this area is evident from 40Ar/39Ar dating approach. The distribution of these basalts may have been controlled by regional tectonics. The age of rock plot shows the older age to the southward since the active extension continued to the northwards. One of evidences is Ko Kra ridge generation in the gulf of Thailand which extends to northward. This occurrence is linked to the rapid up lift of volcanic belt in 11 Ma (Charusiri et al., 1991), the similar age of basalts.

The Cenozoic activity is often claimed as a consequence of continental collision between India and Asia. The different stress with in the crust is resulted in crustal shortening and the movement of strike-slip fault in the area. Then the zones of crustal weakness are formed and characterize by high heat flow. In Eocene, western Burma-Shan Thai collision has occurred. Hence, the thinning of the crust may be trigger. High-temperature basaltic magma may be intrude into the crust causing the crustal partial melting along the weakness zone (Suttirat et al., 1994)

When the hot igneous masses intrude in the weakness zone, the lava may flows on the surface or flow in between layers of rock.

As the lava masses cooling, the joint develop because of the contraction stress on the surface. The cooling prograde directly toward the cooling centers in the middle of the columns and the cracks develop in between each pair of the cooling centers. The cracks distribute over the surface and growth down to the area under the surface. Normally the column are perpendicular to the cooling surface. In basalt flows, there are usually two tires composed of upper colonnade and lower colonnade. These two colonnades meet at quasi-planar interface which are formed by cooling surface above and below the lava masses. At first, initial crack pattern at the surface is not pseudo-hexagonal pattern. The columnar basalt develops step by step, forming from centemeters to decimeters and leaves the traverse band on the side of columnar structure. In well develop columnar basalt, polygonal structure shifts sligthly from crack to one another. The crack continues generating until the isotherm of rock equals to the glass transition temperature. The distances of each crack is lower following the function of thermal gradient.

Unit 6

Conclusion

The fractures in Wichian Buri basalt at Sao-Hin Donsawanare well developing, quite straight, and fracture spacing is about 5 mm. Y-type intersection is the most common intersection, accounting to 70.00%, comparing to the total number of X and T-intersection. There are 3 to 7 sides of polygon for the total of 285 columns in this area. The pentagonal and hexagonal column is the most common. The average diameter size is 40.59 cm. Hexagonality index is 1.06, average number of side is 5.18, and the axial ratio is 1.45. Columnar basalts in this area are slightly weathering and have little porosity around the outer surface. Some columns are tilted at different angle. In the channel, columnar basalt is perpendicular to the ground surface; whereas, columnar basalt near the river bank inclines. There is no undulation of column width. Observing rock texture under light-microscope, Basalt in the study area shows Holocrystalline texture with porphyry. Phenocryst size is about 0.5 mm-5mm and groundmass size is smaller than 0.1 mm. This basalt composes of feldspar50%, opaque mineral 25%, Olivine 10%, Pyroxene 10%, and others 5%. Phenocrysts are pyroxene, olivine, and plagioclase . Texture features are reaction rim of phenocryst, twin in plagioclase, corroded feldspar, and xenolith of mafic mineral. Rock classification by using XRF data, the rock at Sao-Hin Donsawan is mafic rock. This rock can also be classified into alkaline rock and can be further classify into absarokite, alkaline series by using the K_2O vs SiO_2 diagram. By using the total alkali versus silica (TAS) diagram, this rock can be classified into tephrite.

At Sub-Phlu waterfall, the fractures in Wichian Buri basalt are quite poorly developing, curve and unclear, and fracture spacing is about 2 mm. The columnar basalt is not developed well because basalt lava may either heterogeneity or rapid cooling. Y-type intersection is the most common intersection, accounting to 49.30%. There are 3 to 8 sides of polygon for the total of 439 columns in this area. The pentagonal and hexagonal column is the most common. The average diameter size is 31.30 cm. Hexagonality index is 1.33, average number of side is 4.93, and the axial ratio is 1.42. Columnar basalts in this area are slightly weathering and have little porosity around the outer surface. Columns are tilted at same angle. There is little undulation of column width which implies the change of cooling and diverging of growth along the side of column. Observing rock texture under light-microscope, basalt texture is Holocrystalline and porphyry, phenocryst size is about 2 mm-3mm and groundmass size is smaller than 0.1 mm. This basalt composes of feldspar50%,

opaque mineral 25%, Olivine 10%, Pyroxene 10%, and others 5%. Phenocrysts are pyroxene, olivine, and plagioclase grains. Texture features are reaction rim of phenocryst, twin in plagioclase, corroded feldspar. Rock classification by using XRF data, the rock at Sub-Phlu waterfall is mafic rock (45% SiO_2). This rock at Sub-Phlu waterfall can also be classified into alkaline rock and can be further classified into High-K basalt, High-K calc- alkaline series by using the K_2O vs SiO_2 diagram. By using the total alkali versus silica (TAS) diagramcan, the rock can be classified into tephrite to trachy-basalt.

Correlating to previous study, basalt in Amphoe Wichian Buri is Cenozoeic basalt which often interpreted as a consequence of continental collision between India and Asia which is resulted in crustal shortening and weak zones with high heat flow. In Eocene, western Burma-Shan Thai collisions have occurred and trigger the thinning of the crust and High-temperature basaltic magma may be intruded into the crust along the weakness zones. The columnar joint develop because of the contraction stress of lava cooling. The cracks distribute over the surface and growth down to the area under the surface. At first, initial crack pattern at the surface is not pseudo-hexagonal pattern. In well develop columnar basalt, the polygonal structure is formed and crack continues until the isotherm of rock equals to the glass transition temperature.

References

Aydin, A. and DeGraff, J.M., 1988. Evolution of polygonal fracture patterns in lava flows. Science, 239:471-476.

Budkewitsch, P. and Robin, P.Y., 1993. Modelling the evolution of columnar joints. J. Volcanology and Geothermal Research, 59: 219-239.

Charusiri, P. and Pum-Im, S.,2009. Cenozoic Tectonic Evolution of Major Sedimentary Basins in Central, Northern, and the Gulf of Thailand. Bulletin of Earth Sciences of Thailand, Vol.2, No.1&2, p.40-62.

Charusiri, P., Pongsapich, W. and Khantaprab, C., 1990. Granite belts in Thailand: Evidences from the 40Ar/39Ar dating results: The Journal of Scientific Resarch, Faculty of Science, Chulalongkorn University, 16 p.

DeGraff, J.M., and Aydin, A., 1987, Surface features of columnar joints and their significance to mechanics and direction of joint growth. Geological Society of America Bulletin, v. 99, p. 605-6l7.

DeGraff, J.M., Long, P.E. and Aydin, A., 1989. Use of joint growth directions and rock textures to infer thermal regimes during solidification of basaltic lava flows. J. Volcanol.Geotherm. Research, 38: 309-324.

DeGraff, J.M. and Aydin, A., 1993. Effect of thermal regime on growth increment and spacing of contraction joints in basaltic lava. J. Geophys. Research, 98:6411-6430.

Goehring, L. and Morris, S. W., 2008. Scaling of columnar joints in basalt. J. Geophys Research, 113 (B10): 203

Rollinson,H.,1993. Using geochemical data: evaluation, presentation, interpretation.Longman Scientific & Technical. Michigan: Longman Scientific & Technical.

Lucas Goehring, 2003. A Study of 3D Crack Patterns and Columnar Jointing in Corn Starch. Master"s Thesis, Department of Physics, University of Toronto

Phillips, J. C., Humphreys, M. C. S., Daniels, K. A., Brown, R. J., and Witham, F., 2013. The formation of columnar joints produced by cooling in basalt at Staffa, Scotland. Bulletin of Volcanology.75:715-732.

Rateau, R., Schofield, N., and Smith, M., 2012. The potential role of igneous intrusions on hydrocarbon migration, West of Shetland. Petroleumn Geoscience, 19: 259-272.

Saliba, R. and Jagla, E. A., 2003. Analysis of columnar joint patterns from three-dimensional stress modeling. J. Geophysical Research, 108 (B10):2476.

Smrekar, S. E., Moreels, P., and Franklin, B. J., 2002. Characterization and formation of polygonal fractures on Venus. J. Geophysics Research, 107(E11).

Sobolev, V. S., Bazarova, T. Y., and Bakumenko, I.T., 1971. Crystallization temperature and gas phase composition of alkaline effusives as indicated by primary melt inclusions in the phenocrysts. Bullatin Volcanologique, 35(2): 479-496.

Suthirat, C., Charusiri, P., Farrar, E., and Clark, A.H., 1994 New 40Ar/39Ar geochronology and characteristics of some Cenozoic basalts in Thailand: in Proceedings of the International Symposium on Stratigraphic Correlation of SE Asia, IGCP Project 306, Bangkok, Thailand, 15-20 Nov. 1994, p.306-321.

Udinmwen, E., Oden, M. I., Ukwang, E. E., and Edu, E. S., 2016. Structural Geometry of Ikom Columnar Basalt in the Ikom – Mamfe Basin, Southeastern Nigeria. J. Earth and Atmospheric Sciences, 1: 22-29.

Wei, Y., Xu, M., Wang, W., Shi, A., Tang, M., and Ye, Z., 2011. Feasibility of columnar jointed basalt used for high-arch dam foundation. Journal of Rock Mechanics and Geotechnical Engineering, 3(1): 461-468.

Appendix

Data Table: Study area 1

The number of Type- intersection

Table 15. the number of Type-intersection at Sao-Hin Donsawan

Section	T-intersection	X- intersection	Y- intersection
Section 1	16	18	62
Section2	1	13	43
Section3	4	10	35
Section4	4	11	79
Section5	8	12	18
Section6	5	6	30
Section7	6	3	6
total	44	73	273

Calculate average number of side: $h = 2(2JT+3Jy+4Jx)/(Jt+Jy+2Jx)$
By Substitute Type-Intersection value into h-formula yield h=5.18

The number of n-side polygon

Table 16 the number of n-side polygon at Sao-Hin Donsawan

section	3	4	5	6	7	8
Section 1	2	6	36	17	1	0
Section2	0	4	27	17	4	0
Section3	3	5	19	13	4	0
Section4	1	6	18	37	3	0
Section5	0	7	11	4	0	0
Section6	0	3	11	15	1	0
Section7	0	0	6	2	2	0
total	6	31	128	105	15	0

Calculate hexagonality index : $X_N=(f_5+f_7+4(f_4+f_8)+9f_3)^{1/2}$
Where f_n is the function of n-side polygon.
Calculate f_n=n-polygon/total polygon

Table 17. the value of f_n function at Sao-Hin Donsawan

Total polygon	285
f3	0.021053
f4	0.108772
f5	0.449123
f6	0.368421
f7	0.052632

By substitute fn value into formula $X_N=(f_5+f_7+4(f_4+f_8)+9f_3)^{1/2}$
Yield hexagonal index: $X_n=1.06$

Axial ratio

Table 18. Axial ratio value at Sao-Hin Donsawan

Major axis	Minor axis	Axial ratio
45.24	40.77	1.11
45.57	35.17	1.30
38.59	31.88	1.21
44.28	43.40	1.02
38.27	31.79	1.20
44.76	38.92	1.15
63.54	24.11	2.64
45.28	31.42	1.44
36.32	31.29	1.16
36.08	30.19	1.20
41.98	21.60	1.94
59.14	51.51	1.15
39.23	32.57	1.20
32.60	24.57	1.33
29.50	23.87	1.24
46.09	28.13	1.64
42.82	36.24	1.18
28.29	26.52	1.07
31.98	28.59	1.12
28.09	19.44	1.44
38.12	19.25	1.98
34.05	24.95	1.36
38.42	21.37	1.80
36.24	35.72	1.01
48.01	24.82	1.93
48.26	31.40	1.54
56.29	40.74	1.38

Major axis	Minor axis	Axial ratio
45.99	30.45	1.51
25.92	23.52	1.10
35.39	31.81	1.11
51.55	42.86	1.20
37.21	25.50	1.46
42.93	29.51	1.45
45.31	25.62	1.77
40.52	28.33	1.43
28.33	24.86	1.14
30.50	26.83	1.14
30.82	28.77	1.07
51.25	25.99	1.97
37.73	18.50	2.04
32.99	22.84	1.44
56.94	24.49	2.33
52.98	43.43	1.22
37.62	35.51	1.06
54.10	40.99	1.32
58.73	46.69	1.26
45.70	37.35	1.22
46.73	24.93	1.87
40.52	28.79	1.41
46.86	37.43	1.25
45.26	28.61	1.58
57.56	29.13	1.98
57.03	40.13	1.42
58.26	39.98	1.46
58.66	40.68	1.44
52.01	35.95	1.45
52.99	37.07	1.43
52.40	26.09	2.01
60.16	42.76	1.41
61.08	47.50	1.29
61.39	31.98	1.92
53.41	42.68	1.25
42.94	32.54	1.32
39.71	27.50	1.44
42.84	41.49	1.03
48.76	29.94	1.63
51.54	37.32	1.38

Major axis	Minor axis	Axial ratio
42.43	41.85	1.01
50.82	40.32	1.26
50.83	40.65	1.25
48.14	42.11	1.14
48.05	37.03	1.30
35.16	20.92	1.68
28.78	26.97	1.07
43.44	26.17	1.66
36.54	19.24	1.90
45.09	34.77	1.30
45.05	26.37	1.71
49.96	33.78	1.48
44.90	27.29	1.65
43.58	24.73	1.76
35.11	31.16	1.13
40.69	28.36	1.43
35.44	24.52	1.45
31.74	23.29	1.36
49.22	35.89	1.37
38.58	31.80	1.21
44.01	35.75	1.23
41.71	32.53	1.28
46.37	27.48	1.69
39.72	25.39	1.56
42.80	24.38	1.76
41.08	30.76	1.34
40.54	29.28	1.38
39.39	27.33	1.44
41.37	24.60	1.68
41.01	35.58	1.15
44.14	30.75	1.44
45.89	29.77	1.54
51.57	29.14	1.77
60.55	50.75	1.19
39.63	37.25	1.06
49.94	20.94	2.38
37.04	29.21	1.27
43.31	25.82	1.68
38.84	21.89	1.77
40.07	21.53	1.86

Major axis	Minor axis	Axial ratio
43.13	30.85	1.40
49.75	26.32	1.89
69.40	53.80	1.29
54.71	31.96	1.71
33.15	32.80	1.01
43.50	32.83	1.32
55.68	45.29	1.23
58.56	28.31	2.07
64.84	37.95	1.71
51.48	34.84	1.48
59.40	27.24	2.18
73.70	65.80	1.12
75.95	75.47	1.01
73.86	57.94	1.27
66.56	47.73	1.39
63.40	38.55	1.64
65.18	39.96	1.63
56.07	55.96	1.00
62.92	32.94	1.91
94.25	52.32	1.80
65.70	34.80	1.89
66.91	44.53	1.50
61.75	46.82	1.32
48.13	28.27	1.70
62.99	45.07	1.40
58.12	52.84	1.10
52.62	44.99	1.17
51.47	39.37	1.31
60.15	39.00	1.54
49.42	31.69	1.56
50.91	33.88	1.50
38.43	33.04	1.16
38.26	36.35	1.05
49.38	37.53	1.32
48.12	29.62	1.62
44.74	39.08	1.14
	average	1.45
	Axial ratio	1.45

The length of diameter of columnar basalt

Table 19. The length of diameter of columnar basalt at Sao-Hin Donsawan

	min	max	ave	dev
major	25.92157	94.25087	47.3062	11.18294
minor	18.5	75.47474	33.70419	9.434269
axial ratio	1.001946	2.635361	1.447037	0.31511

Data table: Study area2

The number of Type- intersection

Table 20. the number of Type-intersection at Sub-Phlu waterfall

Section	T-junction	X-junction	y-junction
0-1	31	21	53
1--2	20	18	25
2--4	30	27	86
4--6	24	18	48
6--8	17	20	60
8--17	30	18	48
17--end	28	21	85
total	180	143	405

Calculate $h=2(2JT+3Jy+4Jx)/(Jt+Jy+2Jx)$

By Substitute Type-Junction value into h-formula

Yield average number of side: h= 4.93

The number of n-side polygon

Table21 the number of n-side polygon at Sub-Phlu waterfall

Section	3	4	5	6	7	8
0-1	4	11	35	18	2	1
1--2	2	13	14	5	2	1
2--4	5	16	39	16	5	0
4--6	3	11	25	15	1	1
6--8	2	11	18	21	3	2
8--17	4	15	25	16	4	0
17--end	1	10	31	23	6	2
total	21	87	187	114	23	7

Calculate hexagonality index : $X_N=(f_5+f_7+4(f_4+f_8)+9f_3)^{1/2}$
Where f_n is the function of n-side polygon.
Calculate f_n=n-polygon/total polygon

Table 22. the value of f_n function at Sub-Phlu waterfall

Total of column	439
f3	0.047836
f4	0.198178
f5	0.425968
f6	0.259681
f7	0.052392
f8	0.015945

By substitute fn value into formula $X_N=(f_5+f_7+4(f_4+f_8)+9f_3)^{1/2}$

Yield hexagonality index X_n=1.33

Axial ratio

Table 23. Axial ratio value at Sub-Phlu waterfall

Major axis	Minor axis	Axial ratio
32.95	32.61	1.01
32.66	22.73	1.44
29.72	28.47	1.04
29.38	22.94	1.28
26.77	21.45	1.25
42.72	25.56	1.67
28.76	20.88	1.38
41.51	30.75	1.35
39.80	30.94	1.29
37.47	28.87	1.30
28.52	19.25	1.48
22.80	22.50	1.01
33.62	26.50	1.27
30.40	20.38	1.49
28.90	22.91	1.26
34.91	16.84	2.07
37.72	24.17	1.56
21.69	17.54	1.24

Major axis	Minor axis	Axial ratio
20.56	16.39	1.25
34.16	20.16	1.69
37.17	27.34	1.36
44.49	37.28	1.19
40.82	20.24	2.02
40.50	24.10	1.68
38.99	33.85	1.15
43.26	39.95	1.08
42.07	42.07	1.00
50.88	48.44	1.05
47.65	39.72	1.20
39.55	24.25	1.63
26.14	19.26	1.36
27.88	22.15	1.26
24.38	18.25	1.34
23.09	18.27	1.26
54.03	50.43	1.07
14.92	12.74	1.17
51.10	47.24	1.08
22.96	16.30	1.41
25.74	17.04	1.51
20.67	20.03	1.03
28.24	17.37	1.63
28.20	18.94	1.49
47.21	37.52	1.26
42.72	33.08	1.29
58.55	33.66	1.74
47.24	30.04	1.57
45.05	37.47	1.20
35.30	26.89	1.31
39.79	22.84	1.74
37.94	27.38	1.39
33.76	25.28	1.34
33.08	20.11	1.65
38.89	26.52	1.47
33.14	24.46	1.35
44.11	33.20	1.33
32.36	24.03	1.35
23.94	13.01	1.84
31.75	18.92	1.68

Major axis	Minor axis	Axial ratio
36.44	34.34	1.06
39.05	31.77	1.23
44.95	15.17	2.96
39.01	22.71	1.72
37.53	29.19	1.29
45.78	33.37	1.37
31.29	23.52	1.33
31.90	24.44	1.31
29.39	28.45	1.03
27.55	18.80	1.47
43.05	35.10	1.23
34.94	23.01	1.52
23.65	15.82	1.49
47.93	30.80	1.56
35.40	19.14	1.85
43.45	28.49	1.52
24.90	17.21	1.45
39.11	27.32	1.43
51.16	32.67	1.57
48.77	31.05	1.57
57.21	29.07	1.97
38.14	28.66	1.33
29.67	24.40	1.22
45.53	32.19	1.41
43.62	36.42	1.20
39.01	31.55	1.24
50.72	28.49	1.78
38.86	22.10	1.76
37.95	33.69	1.13
35.81	24.33	1.47
33.11	26.78	1.24
29.68	16.99	1.75
29.25	20.48	1.43
27.48	25.66	1.07
50.00	27.26	1.83
38.75	36.16	1.07
40.75	37.30	1.09
36.08	24.51	1.47
31.67	14.18	2.23
23.86	19.22	1.24

Major axis	Minor axis	Axial ratio
21.20	18.56	1.14
44.10	32.40	1.36
30.02	26.13	1.15
25.35	15.76	1.61
40.16	18.24	2.20
38.46	29.60	1.30
52.00	33.92	1.53
44.61	37.93	1.18
36.53	26.19	1.39
41.54	36.26	1.15
36.85	23.04	1.60
33.84	22.43	1.51
43.48	20.43	2.13
47.77	32.32	1.48
41.47	21.21	1.96
27.47	20.07	1.37
27.79	18.72	1.48
28.90	22.41	1.29
36.79	22.01	1.67
36.50	29.07	1.26
40.45	37.22	1.09
37.13	24.20	1.53
24.41	15.44	1.58
26.00	20.57	1.26
31.80	28.54	1.11
33.80	32.90	1.03
44.75	30.57	1.46
55.54	39.10	1.42
43.30	33.04	1.31
28.91	25.41	1.14
29.16	19.13	1.52
40.33	29.57	1.36
42.07	29.63	1.42
34.51	33.17	1.04
49.00	27.34	1.79
33.68	19.51	1.73
24.19	21.24	1.14
33.74	24.84	1.36
35.53	21.48	1.65
35.70	22.24	1.61

Major axis	Minor axis	Axial ratio
35.18	16.86	2.09
28.36	23.52	1.21
37.80	28.36	1.33
35.46	31.38	1.13
24.03	22.99	1.05
36.18	32.98	1.10
32.16	22.73	1.42
31.54	19.84	1.59
31.98	22.31	1.43
30.61	24.72	1.24
35.94	28.80	1.25
23.08	17.04	1.35
36.45	30.84	1.18
45.97	33.90	1.36
42.63	34.29	1.24
33.23	20.82	1.60
54.35	34.89	1.56
30.58	23.81	1.28
28.04	17.75	1.58
37.72	31.46	1.20
28.74	15.10	1.90
42.21	29.99	1.41
36.64	18.89	1.94
43.13	31.41	1.37
34.79	18.89	1.84
45.31	29.33	1.54
40.15	29.08	1.38
42.14	26.15	1.61
55.39	28.03	1.98
32.67	26.55	1.23
45.89	32.79	1.40
38.48	29.34	1.31
37.18	30.84	1.21
24.96	20.99	1.19
41.05	29.19	1.41
37.67	20.48	1.84
35.05	24.63	1.42
	total	1.42

The length of diameter of columnar basalt

Table 24. The length of diameter of columnar basalt at Sub-Phlu waterfall

	min	max	ave	dev
major	14.92387	58.55242	36.36404	8.342088
minor	12.74145	50.42737	26.24404	7.079815
axial	1	2.962453	1.423213	0.286287